

# Effects of octanol on the main transition in model lipid membranes

Peter Dahl Nissen

2<sup>nd</sup> June 2006

Bachelor Project  
Membrane Biophysics Group  
Niels Bohr Institute  
University of Copenhagen  
Supervisor: Thomas Heimburg

## **Abstract**

The role of the cell membrane in the action of anaesthetics is 100 years after it was first brought up still a point of debate. Some believe the membrane to be the site of anaesthetic action, and others believe that proteins are the sites of anaesthetic action.

In this study the effects of the anaesthetic molecule octanol on the main transition in multilamellar model lipid membranes are investigated. A thermodynamical calculation of the effect on the melting temperature is performed and held up against the measured effect. Also, a possible correlation between enthalpy of the system and conformational order of the lipid chains is investigated. Finally, the behaviour of the octanol in the membrane is addressed.

The study is performed on dimyristoylphosphatidylcholine (DMPC) and deuterated distearoylphosphatidylcholine (dDSPC) using differential scanning calorimetry (DSC) and Fourier transform infrared (FTIR) spectroscopy.

It is found that octanol lowers the melting point and broadens the transition regime in the membranes. The measured lowering in melting temperature is smaller than the theoretically predicted, but has a linear relationship with mol% octanol in the membrane as predicted by theory. Further investigations are needed to conclude anything regarding the behaviour of octanol in the membrane and the correlation between enthalpy and conformational order.

<b>1</b>	<b>INTRODUCTION.....</b>	<b>5</b>
<b>2</b>	<b>MATERIALS AND METHODS.....</b>	<b>10</b>
2.1	MATERIALS .....	10
2.2	SAMPLE PREPARATION .....	10
2.3	FTIR MEASUREMENTS .....	11
2.3.1	<i>Data Treatment</i> .....	13
2.4	DSC MEASUREMENTS.....	14
2.4.1	<i>Data Treatment</i> .....	15
2.5	ESTIMATE OF ERRORS .....	15
<b>3</b>	<b>THEORY .....</b>	<b>16</b>
3.1	COLLIGATIVE THERMODYNAMICS.....	16
3.1.1	<i>Calculating enthalpy and heat capacity</i> .....	18
<b>4</b>	<b>RESULTS .....</b>	<b>19</b>
4.1	EFFECT OF OCTANOL ON TRANSITION .....	19
4.2	FTIR MEASUREMENTS AND THEIR CORRELATION WITH DSC MEASUREMENTS .....	22
4.3	BEHAVIOUR OF OCTANOL IN THE MEMBRANE .....	25
<b>5</b>	<b>DISCUSSION .....</b>	<b>27</b>
<b>5</b>	<b>DISCUSSION .....</b>	<b>27</b>
<b>6</b>	<b>CONCLUSION.....</b>	<b>30</b>
<b>7</b>	<b>REFERENCES.....</b>	<b>32</b>
<b>8</b>	<b>APPENDIX .....</b>	<b>35</b>

## List of abbreviations

DMPC	dimyristoylphosphatidylcholine
DSPC/dDSPC	distearoylphosphatidylcholine/deuterated distearoylphosphatidylcholine
DPPC	dipalmitoylphosphatidylcholine
DPPE	dipalmitoylphosphatidylethanolamine
FTIR	Fourier transform infrared
DSC	Differential scanning calorimetry

# 1 Introduction

Even though the effects of anaesthetics on the human body have been known for more than 100 years, the mechanism by which anaesthetics work remains unknown. This is remarkable, considering the simplicity of the mechanism suggested by the relation of the effect of an anaesthetic to its partition coefficient between oil and water (Figure 1.1).

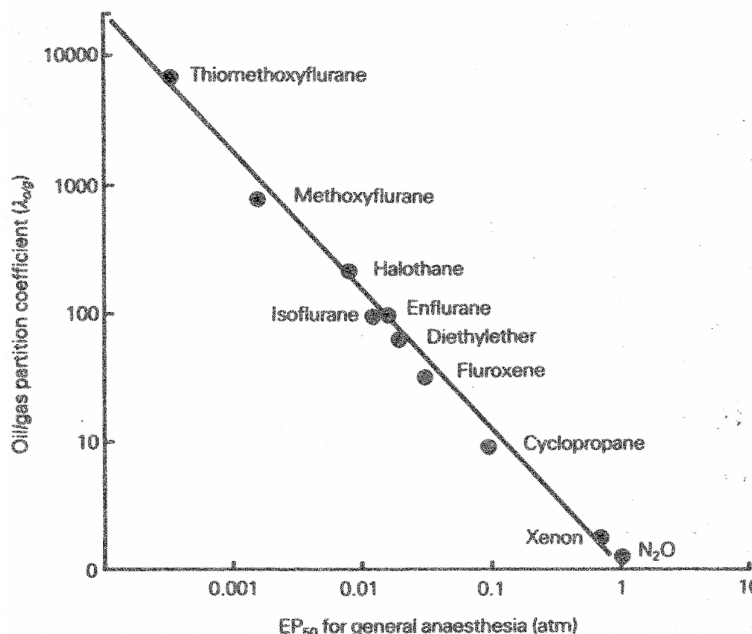


**Figure 1.1:** The Meyer-Overton correlation. The oil/gas partition as a function of potency ( $EP_{50}$ ) for a number of different anaesthetics compounds. [20]

The basis of this thesis is the believe that the target of anaesthetics is the lipid membrane of the cell, inducing a shift in the melting temperature of the membrane which leads to anaesthesia. To investigate this possibility, I have measured the effect of the anaesthetic octanol on the melting temperature of model membranes.

Membranes in the cell are composed of a lipid matrix with embedded proteins. Lipids are small amphiphilic molecules made up of a hydrophilic head group and a hydrophobic hydrocarbon region, see Figure 1.2.

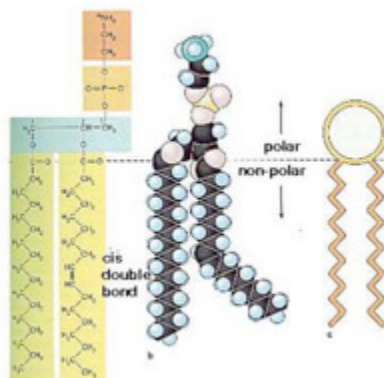


**Figure 1.2:** Schematic representation of a lipid molecule. [37]

Because of their amphiphilic nature lipids dissolved in water can spontaneously form bilayer membranes [2]<sup>1</sup>. It is a bilayer membrane that makes up the cell membrane.

The most accepted model of the cell membrane, proposed by Singer and Nicholson in 1972 [4], states that the proteins diffuse freely in a fluid-like lipid bilayer. This model has over the last decades been modified to incorporate the possibility of local ordered domains of lipids affecting the function of the proteins (Figure 1.3).

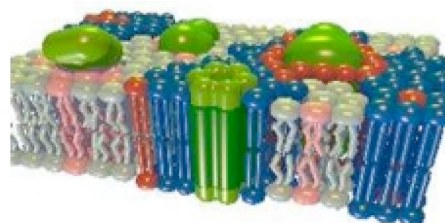


**Figure 1.3:** Model of lipid bilayer membrane showing the ordered domains [38].

Functional domains would explain the need for the thousands of different lipids found in the membranes of the cell – a single membrane is composed of some 500-1000 different kinds of lipids [5]. The differences in for instance head group charge and hydrocarbon chain length affect the physical properties of the lipids and by that the thermodynamic properties of the membrane. The membranes in different cell types differ in composition of lipids and proteins, determining the function of the cell [2].

The complexity of a biological membrane makes for so many independent variables that it is common to use artificial membranes, when studying the physical properties of membranes. Typically these artificial membranes are prepared from a single or two synthetic lipid species [3], [6]-[12]. In this study, artificial membranes of either pure 1,2-dimyristoyl-*sn*-glycero-3-phosphatidylcholine (DMPC) or pure deuterated 1,2-distearoyl-d70-*sn*-glycero-3-phosphatidylcholine (dDSPC) were used. DMPC consists of a phosphatidylcholine head group and two saturated 14-membered hydrocarbon chains, and dDSPC only differ from this in that its hydrocarbon chains contain 18 carbon atoms (Figure 1.4).

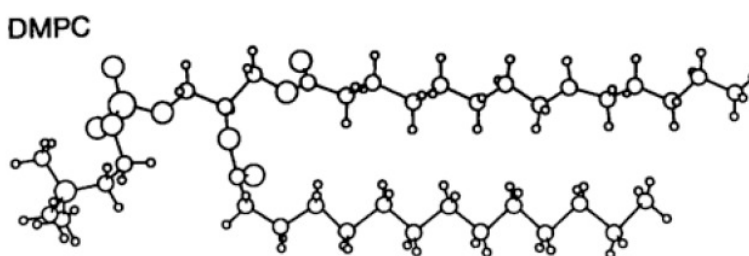


**Figure 1.4:** Structure of DMPC [2]

The hydrocarbon chains in the studied lipids can have various configurations, due to rotations around the C-C bonds – of course such rotation would not take place around double bonds if present. The configuration of a single bond can either be *trans* or *gauche*. The *trans* configuration is the lowest in energy, but the *gauche* configuration has a higher degeneracy, and thereby higher entropy. See Figure 1.5. Therefore the *gauche* configuration becomes more favourable with

---

<sup>1</sup> Other structures may also form dependent on the lipid characteristics such as head group/chain size ratio and the conditions under which they form, e.g. low water content [3].

increasing temperature, implying a possible transition. The lipid chains will start in an all-*trans* conformation at low temperatures, but with increasing temperature more and more *gauche* rotations will be introduced. Eventually at very high temperatures the entropic term is dominant, and *trans* and *gauche* are equivalent from an energetic viewpoint, resulting in a disordered chain [2].

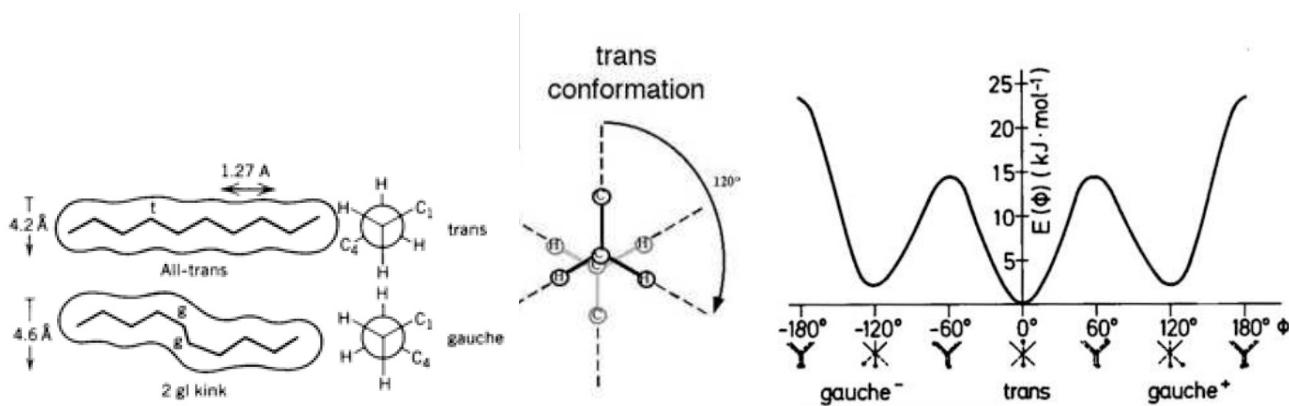


**Figure 1.5:** Schematis representation and energy of *trans* and *gauche* conformers. [2]

The changes in the conformational order of the lipid chains with rising temperature result in transitions between different states/phases of the membrane. Four different states of DSPC and DMPC membranes have been found and characterized [13], [6]. See Figure 1.6. These states are from low to high temperature: the ordered crystalline phase ( $L_c$ ), the ‘gel’-phase ( $L_\beta$ ), the ‘ripple’-phase ( $P_\beta$ ) and finally at highest temperatures the liquid crystalline phase or the ‘fluid’ phase ( $L_\alpha$ ). The three transitions  $L_c \rightarrow L_\beta$ ,  $L_\beta \rightarrow P_\beta$  and  $P_\beta \rightarrow L_\alpha$  are called the sub- pre- and main transition, respectively [6]. The transitions between the different phases occur at defined temperatures dependent on the lipid species. For the lipids in this study at the temperatures of the measurements only the main transition and occasionally the pre-transition are observed.

If we assume that the lipid exists in only two states, all-*trans* and disordered, the melting temperature of the membrane,  $T_m$ , is defined as the temperature, where the two states are found with equal probability [2]. The melting temperature,  $T_m$ , relates to the main transition, and in the following there will only be differentiated between above and below this transition. Above will be referred to as ‘fluid’ and below as ‘gel’, even though the main transition takes place between the ‘ripple’ state membrane and the fluid state.

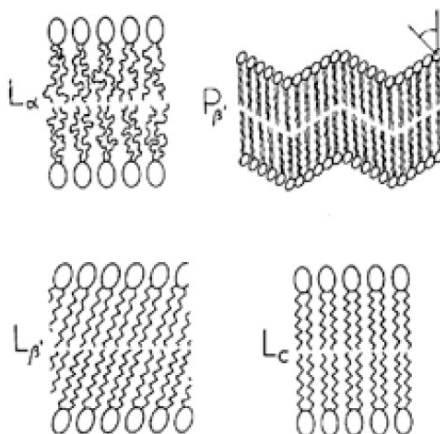


**Figure 1.6:** The different states of lipid membranes. [2]

The chain melting in the lipids result in kinks in the hydrocarbon chain, so that the melted lipid will be shorter, but more bulky than the extended, all-trans lipid [2]. The mismatch between ordered and disordered lipid means that there will be energy associated with an interface between ordered and disordered lipids. Since the lipids melt gradually during the transition from gel to fluid, interfaces between ordered and disordered lipids will be present [14], [9], [2]. To minimize the energy, the system separates into domains of ordered and disordered lipids, thereby decreasing the interface area. The size of the domains will depend on how large the interaction energy is; for very large interaction energy the domain will be as large as regular phases, whereas no interaction energy will allow the lipids to mix randomly, and no domains will form [14], [2]. This interaction energy is also what causes the cooperativity seen in transitions [6], [12], [14]. Cooperativity means that all the lipids melt almost at the same time – this happens since interfaces between ordered and disordered lipids thereby become minimal.

To summarize, the sharpness of the transition depends on the magnitude of the interaction energy between ordered and disordered lipids. Small interaction energy would result in an uncooperative transition, and vice versa for large interaction energy.

It is an experimental fact, that the cooperativity of the membrane transition can be greatly diminished by addition of anaesthetics to the membrane [9], [15]. Besides decreased cooperativity many other effects of anaesthetics on the physical behaviour of membranes have been measured. Most of them follow from the lowering of the melting point, which is the main effect anaesthetics have on membranes [8]-[10], [12]. Some of these effects are increased membrane fusion (increased elasticity) [16], increased permeability [16], [17] and expansion [16], [18]. Thus, the mechanical properties of the membrane can be greatly influenced by anaesthetics. Interestingly, the effects of different anaesthetics on the physical behaviour of the membrane are the same, despite their very different chemical structure [16] (Figure 1.7). This observation resembles one made more than 100 years ago.

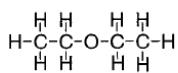
**Volatile anaesthetics and anaesthetic gases**



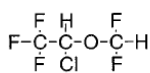
**Chloroform**



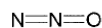
**Halothane**



**Diethyl ether**



**Isoflurane**

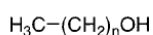


**Nitrous oxide**

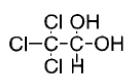


**Xenon**

**Alcohols**

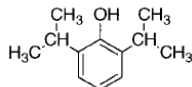


**n-alcohols**

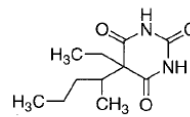


**Chloral hydrate**

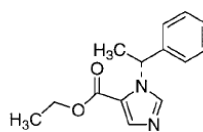
**Intravenous anaesthetics**



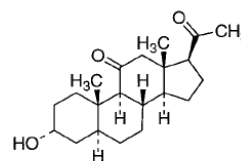
**Propofol**



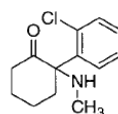
**Pentobarbitone (a barbiturate)**



**Etomidate**



**Alphaxalone (steroidal anaesthetic)**



**Ketamine**

**Figure 1.7:** Different anaesthetics, divided into groups. [36]



At the turn of the last century it was independently observed by Meyer (1899) [19] and Overton (1901) [20] that the potency of an anaesthetic correlated with its partition coefficient between olive oil and water, the so called Meyer-Overton-correlation, Figure 1.1. This led them to propose a ‘model’ for anaesthetic action based on interactions with lipids in the cells changing their physical state [21] – this was before the concept of a cell membrane was developed. Based upon Meyer and Overton’s statements, a theory evolved, that the mechanism of anaesthetic was to dissolve in the membrane, causing a change in its physical state which would alter the function of membrane bound proteins. This mechanism was universally accepted for more than 60 years.

However, with time numerous exceptions from the Meyer-Overton-correlation were observed. In addition, observations of anaesthetics binding directly to a hydrophobic pocket of firefly luciferase (reviewed in [22]) as well as different potencies of stereoisomers of anaesthetic compounds [22] supported the idea that anaesthetics interact with proteins directly presented by Franks and Lieb’s [23].

Still today the ideas of Overton-Meyer and Franks-Lieb are the basis of many studies, but as of yet no final piece of evidence for a mechanism has been presented. Thus there is still need for new experiments that will shed light on the mechanism of anaesthetics. I believe that these experiments need to focus on the effects of anaesthetics on the main transition in membranes.

Evidence exists that membranes in biological systems are within few degrees of their phase-transition temperatures (Figure 1.8) [2]. This could be taken as an indication of that the organism exploits the dependence of the melting point on controllable conditions such as pH and ionic strength to move in and out of the transition regime to switch signalling processes on and off.

In such an event anaesthetics could act by shifting the transition temperature out of the temperature range attainable by shifts in pH and ionic strength.

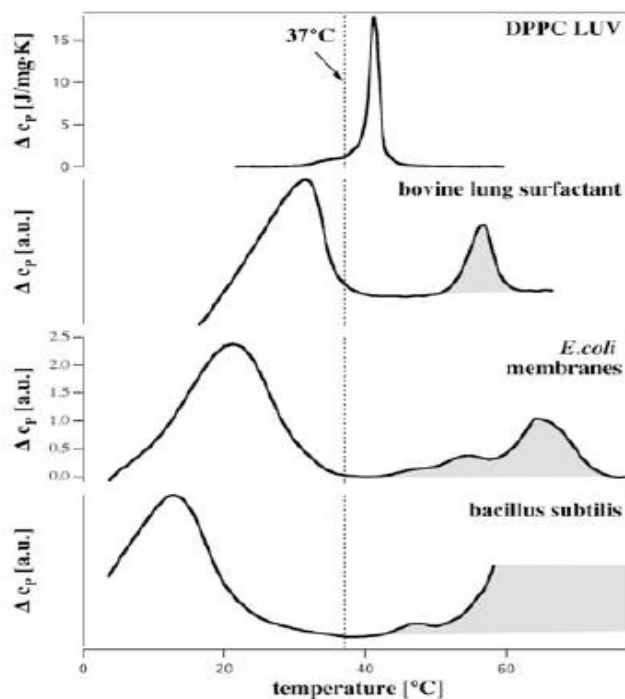


**Figure 1.8:** Melting of lipid membranes in artificial system and various biological systems. [2]

These thoughts act as motivation for measuring the dependence of the phase-transition temperature in model membranes on anaesthetics. The goal of this study is to perform these measurements and compare them with theoretical predictions based on a thermodynamic approach. Also the behaviour of the anaesthetic in the membrane should be measured, to test the assumption made about this in the theoretical treatment.

The question could then be: How do we measure the transition in a membrane and how do we know what the different states of the membrane look like?

A plethora of different physical techniques have been used to study these things such as infrared spectroscopy, X-ray diffraction, neutron scattering, electron microscopy, NMR spectroscopy, calorimetry, fluorescence correlated spectrometry, densimetry, and atomic force microscopy. The different techniques are sensitive to different parameters and structural changes, so that they collectively allow investigation of almost any feature of the membrane and events therein.

In this study, I have used differential scanning calorimetry (DSC) and Fourier transform infrared spectroscopy (FTIR spectroscopy) to measure the effect of anaesthetics on the main transition. The two techniques measure the transition through different parameters, and a possible linear correlation between the parameters will be investigated. Further DSC has the ability to obtain thermodynamical data needed in the theoretical calculations, and with FTIR spectroscopy it is possible to separately observe lipid and anaesthetic using deuterated probes.

## 2 Materials and Methods

### 2.1 Materials

Both DMPC and dDSPC were obtained from Avanti Polar Lipids and used without further purification.

### 2.2 Sample preparation

All lipid solutions were made by mixing appropriate amounts of lipid and H<sub>2</sub>O, by weighing the lipid and pipetting the water.

The DMPC in the solutions containing 5, 10 and 15 mol% octanol in the membrane had prior to being dissolved in water been solvated in a 2:1 mixture of dichloromethane/methanol solution. This solvent was evaporated in a water bath (50°C) under a light stream of N<sub>2</sub>, and placed in dessicator overnight to remove all traces of solvent. This procedure was unnecessary, but should not in any way affect the results of the measurements.

The amounts of octanol needed to obtain the wanted mole fractions in the membranes were calculated based on rough estimates of the partitioning coefficients for octanol between the respective lipid and water,  $K_{L/W}$ . The estimates were obtained in the following manner.

The partitioning coefficient for octanol between dipalmitoylphosphatidylcholine (DPPC) and water,  $K_{DPPC/W}$ , was obtained from a communication [11]. Although this supposedly was for partitioning of octanol into gel-phase DPPC it was used in further calculations as a general partitioning coefficient. From an article [24], a partitioning coefficient for octanol between DPPC and DMPC was obtained,  $K_{DMPC/DPPC}$ . This partitioning coefficient was based on a theoretical thermodynamic calculation using many approximations, and was not supposed as an estimate of the real value of this partitioning coefficient. Despite this the value was used together with the value of  $K_{DPPC/W}$  to get a value for  $K_{DMPC/W}$  in the following manner,

$$K_{DMPC/W} \equiv \frac{c_{octOH,DMPC}}{c_{octOH,W}} = \frac{c_{octOH,DMPC}}{c_{octOH,DPPC}} \cdot \frac{c_{octOH,DPPC}}{c_{octOH,W}} = K_{DMPC/DPPC} \cdot K_{DPPC/W}$$

where  $c_{octOH,DMPC}$  denotes the concentration of octanol in the DMPC membrane. From this a value of 176 for  $K_{DMPC/W}$  was obtained.

$K_{DSPC/W}$  was estimated based on the observation that partition coefficients increase monotonically with lipid chain length [11]. Since the chain lengths for DMPC, DPPC and DSPC are 14, 16 and 18, respectively  $K_{DSPC/W}$  was estimated to 220.

As the amounts of octanol needed were on the order of  $0.1\mu\text{L}$  it was not possible to pipette directly. Instead a larger amount of octanol was dissolved in methanol and water and an aliquot amount (usually on the order of  $5\mu\text{L}$ ) of this solution was added to the lipid solution. The methanol was used to dissolve a larger amount of octanol in water. Since methanol is known to practically not go into the membrane (as can be seen from the trends in [25]), the added amount of methanol is expected not to perturb the system significantly.

An exception from this procedure was the dDSPC solutions. Here the octanol was added from a  $1.90\text{ mM}$  solution of octanol in water.

After addition of octanol the samples were shaken mechanically, heated to  $\sim 20^\circ\text{C}$  above their transition temperature for 10 minutes, shaken mechanically while warm and allowed to cool well below the transition temperature. This procedure was repeated three times to ensure complete hydration of the sample.

The sample was either used directly or stored for up to 3 days at  $5^\circ\text{C}$ . Storing for this period should have no effect on the main transition [6].

### 2.3 FTIR Measurements

Infrared spectroscopy is a commonly used technique to measure structural changes in for instance lipid membranes [6], [26].

The heart of the FTIR spectrometer is a Michelson interferometer with a moving mirror. Light from the source is split into two beams by a half-silvered mirror; one is reflected off a fixed mirror and one off a moving mirror which introduces a time delay. Figure 2.3.1.

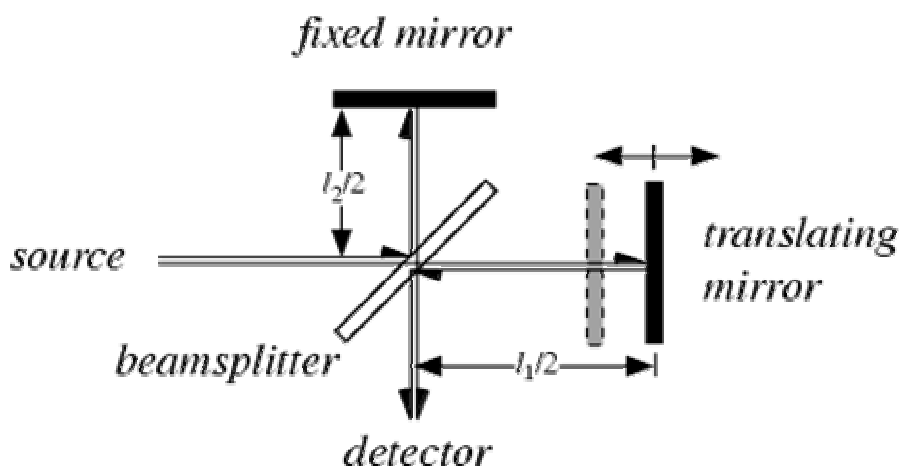


Figure 2.3.1: Michelson interferometer with moving mirror. [27]

By smoothly translating one mirror, the optical path difference between the beams reflecting off the two mirrors is varied continuously, producing an interferogram. Then by taking the Fourier transform of the interferogram the spectrum is obtained [27].

In this study the spectral regions of interest are the  $3000\text{-}2800\text{ cm}^{-1}$  and  $2200\text{-}2000\text{ cm}^{-1}$  regions, where the  $\text{CH}_2$  and  $\text{CD}_2$  symmetric and antisymmetric stretching bands are, respectively. See Figure 2.3.2.

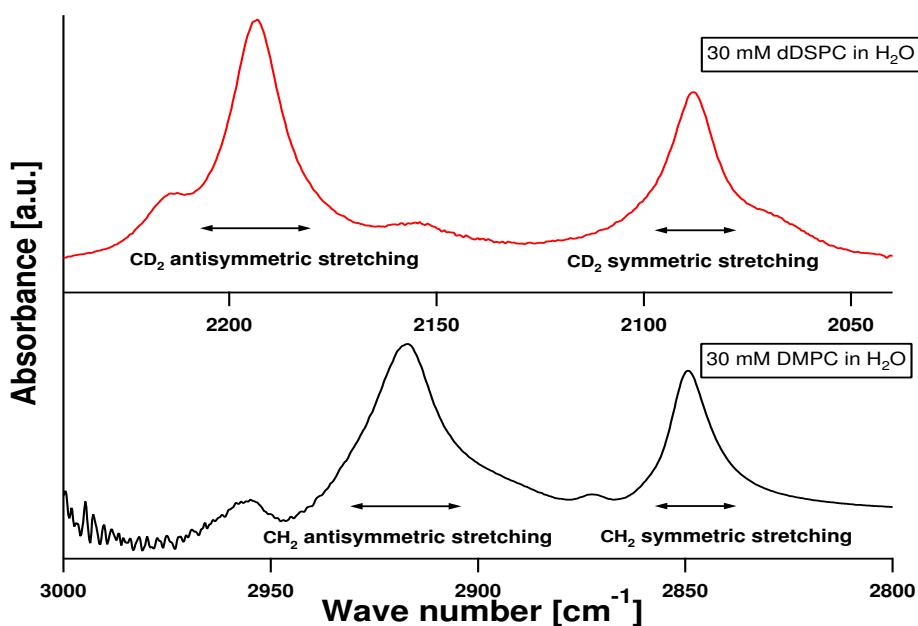


Figure 2.3.2:  $\text{CH}_2/\text{CD}_2$  symmetric and antisymmetric stretching

The wavenumber of these bands is sensitive to *trans/gauche* ratio in the lipid chains, making them sensitive to the transition in the membrane.

In Figure 2.3.3 the recorded spectrum of DMPC in H<sub>2</sub>O is shown. As can be seen in the Figure 2.3.3, the  $\text{CH}_2$  symmetric stretching band at  $2850\text{ cm}^{-1}$  is less overlapped by the water band than the antisymmetric band at  $2920\text{ cm}^{-1}$ . Therefore we choose to measure the position of the symmetric

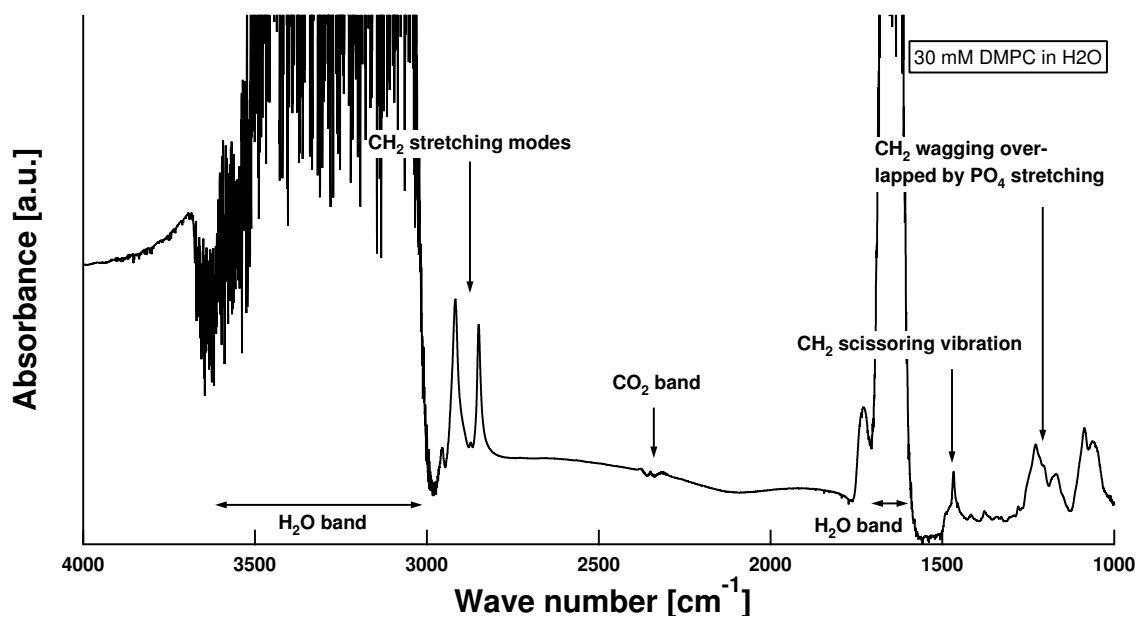


Figure 2.3.3: Infrared spectrum of DMPC in H<sub>2</sub>O showing the characteristic peaks.

stretching band. In the measurement with dDSPC and octanol we use the symmetric band at  $2090\text{ cm}^{-1}$  to characterise the state of the dDSPC and the symmetric stretching band at  $2850\text{ cm}^{-1}$  to characterise the state of the octanol.

Other bands in the spectrum shown in Figure 2.3.3 can also yield information about the membrane. Examples are the  $\text{CH}_2$  scissoring band at  $1470\text{ cm}^{-1}$  and the  $\text{CH}_2$  wagging band at  $1200\text{ cm}^{-1}$  [6], [7].

All spectra were recorded at a resolution of  $0.50\text{ cm}^{-1}$  on a VERTEX 70 FT-IR spectrometer from Bruker Optics equipped with a KBr beam splitter.

For FTIR measurements samples were placed between two  $\text{CaF}_2$  windows separated by a  $50\mu\text{m}$  Teflon spacer in a homemade housing connected to a thermo bath controlled by a computer. The macros for the measuring procedure were written in OPUS (Software supplied by manufacturer). Both the measuring and the detector chambers were purged with  $\text{N}_2$  gas and the detector was cooled with liquid  $\text{N}_2$ . Measurements were performed at least 30 min after initiation of purging. 32 scans were performed for each of the recorded spectra, both sample and background. These interferograms were added and Fourier transformed using a Blackman-Harris 3 Term apodization function.

Temperature correlation measurements were performed using a thermocouple wire inserted between the  $\text{CaF}_2$  windows separated by a  $\sim 1\text{ mm}$  thick rubber spacer.

### 2.3.1 Data Treatment

Data analysis was performed with both OPUS software (supplied by manufacturer) and Igor Pro (WaveMetrics). With OPUS the position of the  $2850\text{ cm}^{-1}$  peak was determined by the peak position determining function. The spectrum had previous to this been Fourier deconvoluted in the region of the peak using a Lorentzian line shape with a deconvolution factor of 10000 and a noise reduction factor of 0.5. This was done to sharpen the peak [34].

In Igor the peak was fitted with a second degree polynomial to improve the spectral resolution and

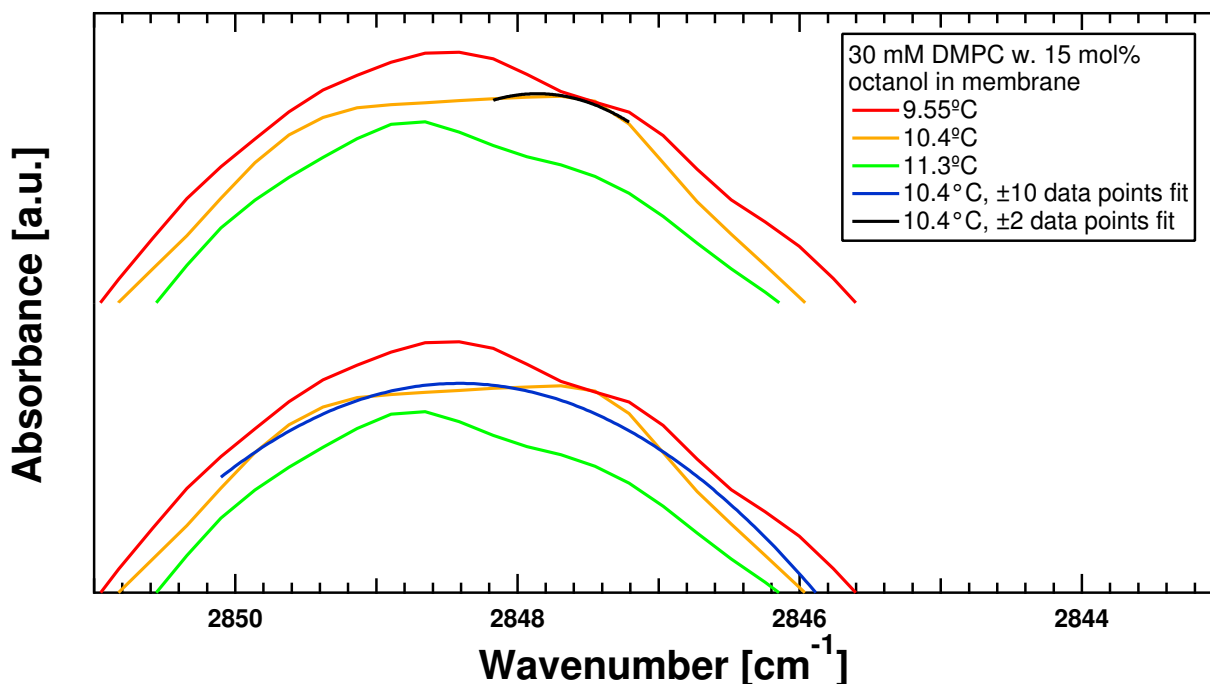


**Figure 2.3.1.1:** Peak of the  $2850\text{ cm}^{-1}$   $\text{CH}_2$  symmetric stretching band for three temperatures. Also shown, the second degree polynomial fits to a region of 10 and 2 data points to each side of the top point of the peak.

to eliminate the effect of noise in the spectra. The fit was performed on a spectral region of 10 data points to each side of the peak, as determined from the spectral data. This is illustrated in Figure 2.3.1.1. A fit with  $\pm 10$  data points was found to be optimal by trial and error. As seen in Figure 2.3.1.1 a fit using  $\pm 2$  data points was not able to eliminate the effect of noise in the spectrum. A fitting procedure with a third degree polynomial was tested, but yielded the same results.

From the plots of the fitted peak positions as a function of temperature, the temperatures of the onset, midpoint and completion of the phase transition were determined. The upper and lower transition temperature was found by determining the intersections of the straight lines that can be drawn through the three distinct portions of each curve. See Figure 2.3.1.2.

Placement of the line on the mid portion of the curve became increasingly error prone with increasing amounts of alcohol. The transition temperature was determined as the temperature corresponding to wavenumber given by the mean of the wavenumbers corresponding to the upper and lower transition temperature.

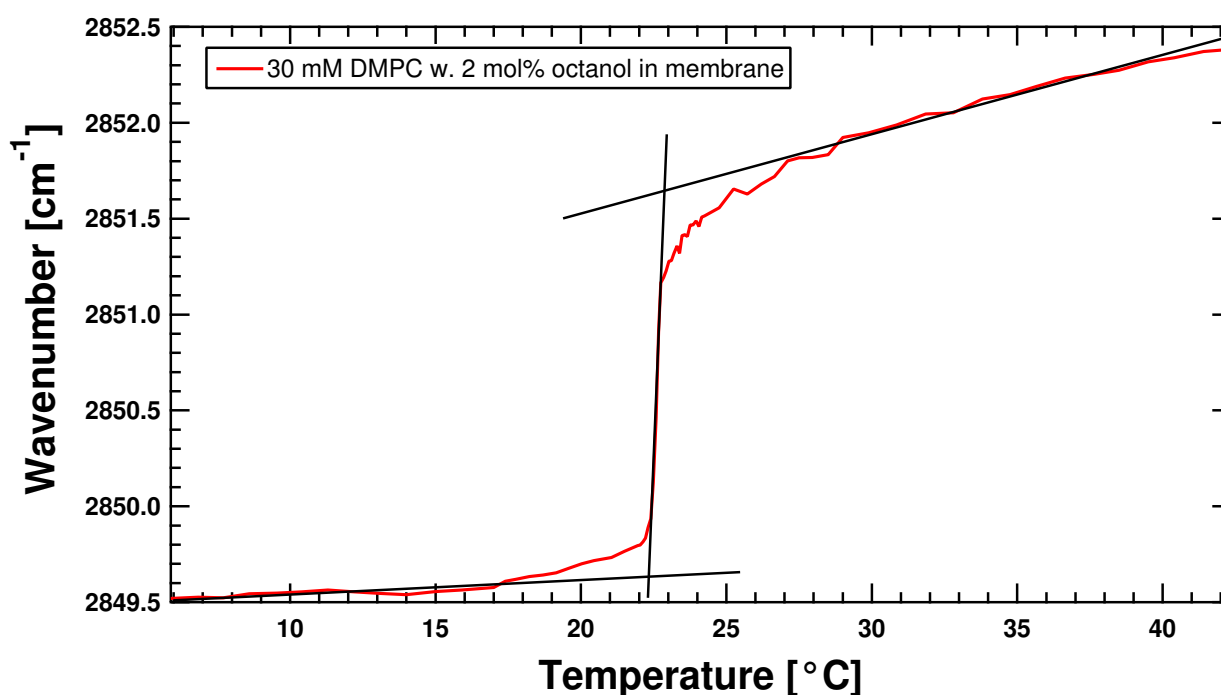


Figure 2.3.1.2: Method for estimating upper and lower transition temperature from graph.

## 2.4 DSC Measurements

A DSC consists of two separate thermally isolated chambers. One chamber holds the sample and the other contains a reference, in this case DMPC and water, respectively. Under conditions of constant pressure, the two chambers are heated at a given rate. The DSC measures the heat needed to warm up the sample to a given temperature relative to the heat needed for the reference to reach the same temperature. The differential of extra heat per temperature increment gives the heat capacity of the sample.

All scans were performed on a Microcal VP-DSC in a temperature range of 10°C to 35°C with a scan rate of 5°C/hour.

### 2.4.1 Data Treatment

The obtained heat capacity data were transferred into Igor Pro. A fit of the baseline of the heat capacity profile was obtained from the region of the profile not containing the peak associated with the transition. By subtracting the baseline, the heat capacity of the transition alone is obtained, and the ‘background’ heat capacity of the lipids is left out.

The biggest problem with this procedure is the fitting of the baseline, since it can be hard to estimate how large a portion of the data you need to delete to leave out the transition peak without removing the validity of the fit. See Figure 2.4.1.1.

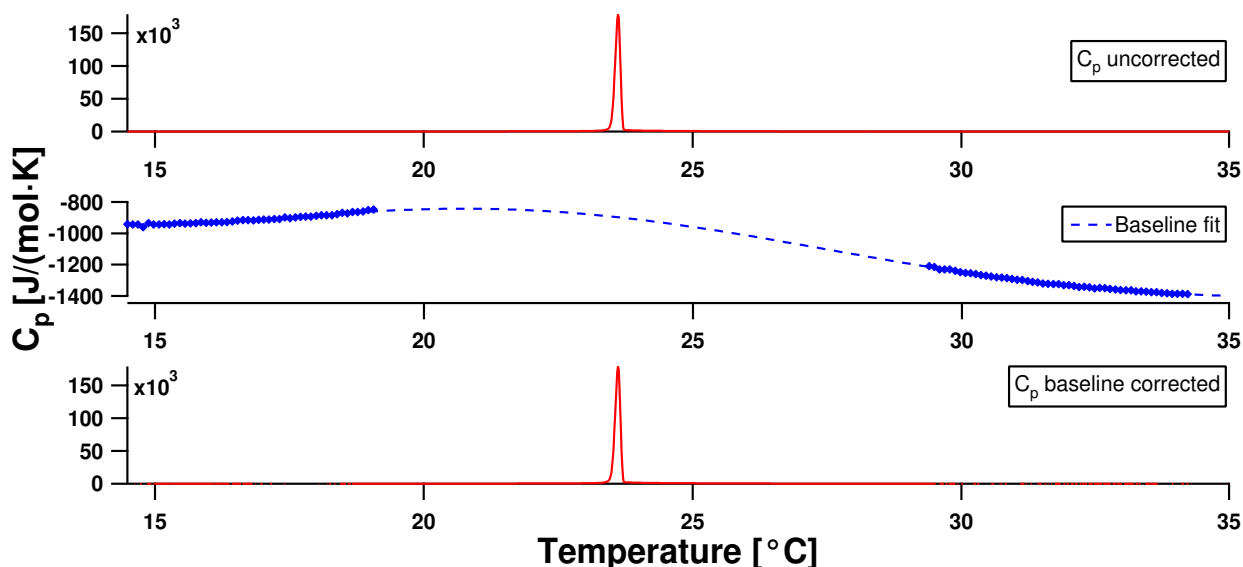


**Figure 2.4.1.1:** Procedure for baseline subtraction. Upper: Uncorrected heat capacity profile. Middle: Estimation of baseline. Lower: Baseline corrected heat capacity profile.

The calculation of the measured enthalpy was done by integrating the entire temperature range of the baseline corrected heat capacity profile. The advantage with this integration range is the consistency in it, but if the baseline subtraction was not very good, you could easily overestimate the enthalpy of the transition.

The temperatures of the upper and lower end of the transition were found from the enthalpy profiles as described for the plots of wavenumber vs. temperature. The transition temperature,  $T_m$ , was found as the temperature at which the enthalpy is the half of the end value, in agreement with the definition of  $T_m$ .

### 2.5 Estimate of Errors

An error prone part of the experiments is the sample preparation. The weight had a precision of 0.0001 g, and in general ~0.010 g of lipid was weighed. This is an error of ~1%. In one case, the dDSPC, only 0.0021 g of lipid was weighed, in which case the error was ~5%. Also the pipettes are accurate within about 1%.

The temperature measured by the DSC is very accurate, whereas the temperature measurements made with the thermocouple are only precise within ~0.1°C. The larger the measured shift in transition temperature is, the less influence this uncertainty in temperature will have.

It is hard to estimate the size of the error made in the baseline subtraction of the heat capacity profiles and the graphical estimation of the transition temperatures, but the spread of the results imply, that the error is significant.

It is important to remember, that the uncertainty in the actual mole fraction of lipid is so large, that it dwarf all the other errors.

### 3 Theory

M. W. Hill was in 1974 the first to give a thermodynamic analysis of the observed melting temperature lowering for lipids in the presence of anaesthetics [8]. Here I will introduce the simple model and its assumptions, which lead to surprisingly correct predictions about lowering of melting temperature by especially small molecules such as short chain alcohols, [8], [10].

The following is based on the sources [2], [8] and [10].

#### 3.1 Colligative Thermodynamics

Let us assume that we have a lipid that exists in only two states, gel (l) and fluid (f) and that no interfaces between the lipids in the two states exist.

The Gibbs free energy,  $G$ , for each of the two states is given by

$$G_{g/f} = H_{g/f} + T \cdot S_{g/f},$$

where  $H_{g/f}$  and  $S_{g/f}$  are the enthalpy and entropy for gel/fluid lipids, respectively. We now introduce the chemical potential of the  $i$ 'th component,  $\mu_i$ , as the partial molar Gibbs free energy, defined as

$$\mu_i = \left( \frac{\partial G}{\partial n_i} \right)_{p, T, n_{j \neq i}},$$

meaning the variance in  $G$  when changing the amount of the  $i$ 'th component of the system. If we in addition to the assumption of no interfaces assume ideal mixing between lipids and anaesthetic, the chemical potential is merely the same as the Gibbs free energy per mol

$$G_{g/f} = n_{g/f} \cdot \mu_{g/f}.$$

This leads to the differential

$$(1) \quad dG_{g/f} = V_{g/f} dp - S_{g/f} dT + \mu_{g/f} dn_{g/f},$$

where we neglect the contribution to the energy of the dissolved amount of anaesthetic.

Adding an anaesthetic to the system will result in a change in the pressure because of the change in volume per particle. The molar Gibbs free energy will change as given by

$$(2) \quad \mu_{g/f} = \mu_{0,g/f} + \int_{P_{g/f,0}}^{P_{g/f}} V dp = \mu_{0,g/f} + RT \ln \frac{P_{g/f}}{P_{g/f,0}},$$



using that since the components do not interact with each other, the ideal gas law applies. Furthermore, Raoult's law stating  $p_i = x_i \cdot p_{i,0}$  holds for ideal mixtures by definition, changing equation (2) into

$$(3) \quad \mu_{g/f} = \mu_{g/f,0} + RT \ln x_L^{g/f},$$

$x_L^{g/f}$  denoting the mole fraction of lipid the gel/fluid phase.

In thermal equilibrium between gel and the fluid lipid phase at constant pressure and temperature, the Gibbs free energy is in a minimum implying that the chemical potentials in the two phases are the same. This yields

$$(4) \quad \mu_{g,0} + RT \ln x_L^g = \mu_{f,0} + RT \ln x_L^f \quad \rightarrow \quad \ln \frac{x_L^f}{x_L^g} = \frac{\mu_{g,0} - \mu_{f,0}}{RT} = -\frac{\Delta\mu_0}{RT}.$$

Using that  $\Delta\mu_0 = \Delta H_0 - T\Delta S_0$  and  $\Delta S_0 = \frac{\Delta H_0}{T_{m,0}}$  gives us

$$(5) \quad \ln \frac{x_L^f}{x_L^g} = -\frac{\Delta H_0}{R} \left( \frac{1}{T} - \frac{1}{T_{m,0}} \right).$$

If we now assume that when measuring the temperature in Kelvin, the perturbation in melting point is relatively small, we can make the approximation  $T \cdot T_{m,0} = T_{m,0}^2$  which lets us rewrite (5) as

$$(6) \quad \Delta T = T_{m,0} - T = -\frac{RT_{m,0}^2}{\Delta H_0} \ln \frac{x_L^f}{x_L^g}.$$

A small change in melting temperature will often be associated with a small overall amount of anaesthetic in the membrane, meaning that both  $x_L^f$  and  $x_L^g$  are likely to be small, in which case

$$(7) \quad \Delta T = \frac{RT_{m,0}^2}{\Delta H_0} (x_A^f - x_A^g), \quad \text{using} \quad x_L^f + x_A^f = 1 \quad \text{and} \quad x_L^g + x_A^g = 1.$$

$x_A^f$  and  $x_A^g$  denote the mole fractions of anaesthetic in the fluid and gel phase, respectively.

Going to the extreme case as Hill did, where the anaesthetic is assumed to mix ideally with the fluid phase while being immiscible in the gel phase, we have  $x_L^g = 1$ . With this we obtain from (6)

$$(8) \quad \Delta T = -\frac{RT_{m,0}^2}{\Delta H_0} \ln x_L^f = -\frac{RT_{m,0}^2}{\Delta H_0} \ln(1 - x_A^f) = \frac{RT_{m,0}^2}{\Delta H_0} x_A^f,$$

which is the same as (7) with  $x_A^g = 0$ .

Using a definition of the melting temperature, as the temperature where all of the lipids are in the fluid state we will have the relation  $x_A^f = x_A$ , where  $x_A$  is the mole fraction of anaesthetic in the solution of lipids, both gel and fluid. This allows us to write (8) as

$$(9) \quad \Delta T = \frac{RT_{m,0}^2}{\Delta H_0} x_A,$$

predicting a linear decrease in the melting temperature as a function of anaesthetic mole fraction.

### 3.1.1 Calculating enthalpy and heat capacity

The above models allows one to do theoretical calculations of both the molar enthalpy and heat capacity of the transition as a function of temperature for a given amount of anaesthetic. All you need to know is the molar enthalpy of transition,  $\Delta H_0$ , and the unperturbed melting temperature,  $T_{m,0}$ , of the membrane

To calculate the enthalpy we use the assumption that the absolute enthalpy at a given point during the transition is given by:

$$(10) \quad H(T) = x^g \cdot H_g + x^f \cdot H_f \rightarrow \Delta H(T) = x^f \cdot \Delta H_0,$$

where  $x^g$  and  $x^f$  are the fractional amounts of gel phase and fluid phase and  $H_f$  and  $H_g$  are the absolute molar enthalpies of fluid- and gel-state lipids, respectively. The change in molar enthalpy of the system at given temperature is then as noted in the last equation in (10).

We now use the facts that

$$x_A = x^f \cdot x_A^f \rightarrow x^f = \frac{x_A}{x_A^f}$$

and that we from (5) with  $x_L^g = 1$  can calculate  $x_A^f$  at a given temperature,  $T$ , lower than the melting temperature with the given amount of anaesthetic. With this equation (10) lets us calculate  $\Delta H(T)$ .

From the calculated  $\Delta H(T)$  it is now easy to calculate  $\Delta C_p(T)$ , since we know

$$\Delta C_p(T) \equiv \frac{d\Delta Q(T)}{dT} = \left( \frac{d(\Delta H(T))}{dT} \right)_p.$$

## 4 Results

### 4.1 Effect of Octanol on Transition

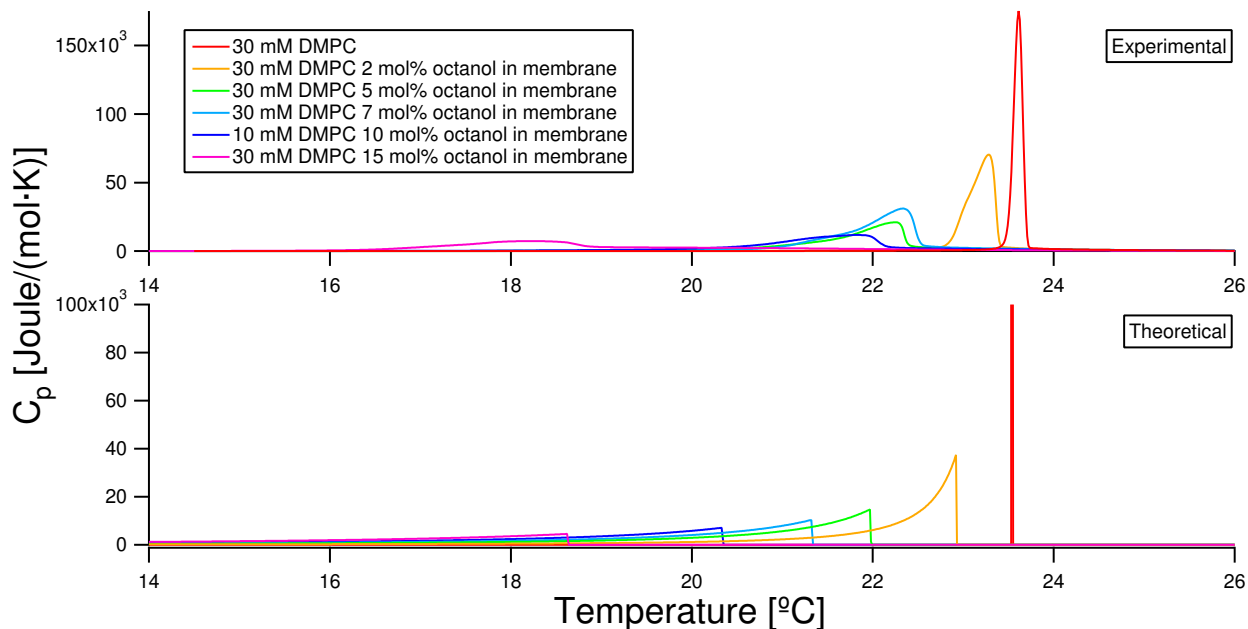


**Figure 4.1.1:** Heat capacity profiles of DMPC membranes with octanol. Both measured and calculated. The calculated heat capacity profile for pure DMPC has been truncated to make the other calculated profiles visible.

From the heat capacity profiles it is obvious that octanol has an effect on the lipid melting (Figure 4.1.1). The profiles broaden and shift downwards in as well height as temperature with increasing percents of octanol in the membrane, features that are qualitatively the same as for the theoretically calculated heat capacity profiles calculated from values found below (Figure 4.1.1). The diminished steepness of the heat capacity profiles reflects a decrease in cooperativity in the transition upon addition of octanol. The reason for this decrease in cooperativity is discussed later. The values of  $T_m$  and  $\Delta H_0$  estimated from the measured heat capacities are found in Table 4.1.1.

mol% octanol in membrane	$T_m$ [°C]	$\Delta H_0$ [kJ/(mol)]
0	23.6	24.7
2	23.1	27.0
5	22.0	22.8
7	22.1	30.6
10	21.5	21.2
15	18.6	21.8

**Table 4.1.1:** Result of DSC scans on solutions of DMPC multilamellar vesicles containing the listed mole-% octanol within the membrane.

As seen, the measured excess enthalpies vary greatly with no apparent correlation with the amount of octanol. Therefore it is very likely, that the variations stem from uncertainties in defining the baseline to subtract from the measured dataset, as described in *Materials and Methods*. The error in neither weighing the lipid nor pipetting the added water can account for the deviations. The mean value of the measured enthalpies is 24.7 kJ/mol, which is somewhat higher than the value of 21.05

kJ/mol referenced in the literature [12]. The melting temperature of 23.6°C of the pure lipid is consistent with values reported elsewhere [12], [28].

Since there seems to be no reason why the enthalpies of the different solutions should differ, the enthalpy profiles have been rescaled to end at 24.7 kJ/mol to ease comparison between them (Figure 4.1.2) and likewise the area under the heat capacity profiles has been normalized (Figure 4.1.2).

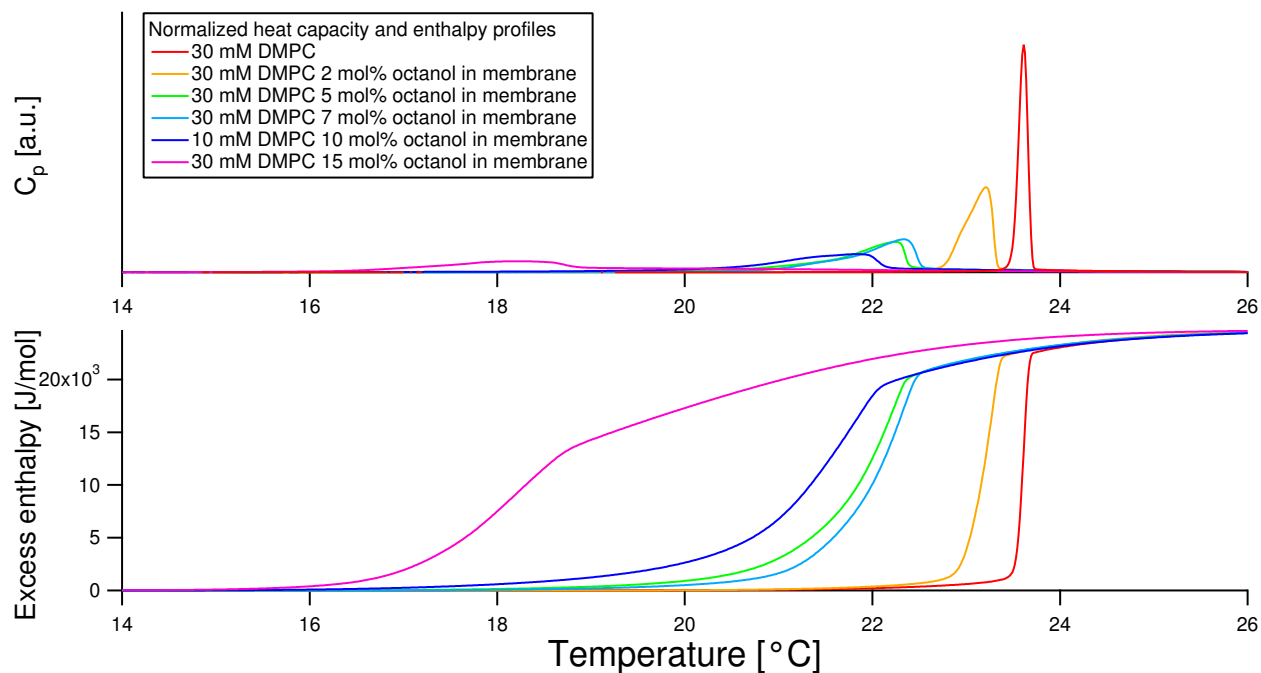


**Figure 4.1.2:** Normalized profiles of excess enthalpy as well as excess heat capacity.

In Figure 4.1.2 it can be seen that the top part of the normalized enthalpy profile of the 15 mol% sample does not follow the same line as all the others. The cause for this alternate curvature can be seen in Figure A.1 in the *Appendix*, where the individual heat capacity profiles are presented. Here we see a shoulder to the right of the main transition peak with a constant height of about 3000 kJ/(mol·K) moving with the transition peak. This peak does not decrease in height as the main transition peak, making it seem like it grows. Since this peak does not decrease and moves with the transition peak, it is likely that it is due to an error in baseline subtraction. Thus the special appearance of the enthalpy profile for the 15 mol% sample is more likely to be caused by poor baseline subtraction than special events in the lipid bilayer with 15 mol% octanol. Attempts to improve the baseline subtraction were unsuccessful.

From the figure 4.1.2 it is also noted, that especially the temperature of the onset of the transition is affected, showing a markedly stronger lowering in response to the octanol than the temperature of the completion of the transition. The temperatures of the onset,  $T_o$ , and completion,  $T_c$ , of the transition have been estimated from Figure 4.1.2 as described in *Materials and Methods* and the variation of these with amount of octanol in the membrane is listed in Table 4.1.2. These temperature values are plotted in Figure 4.1.3 along with the  $T_m$  dependence on octanol concentration, and a the theoretical dependence of the melting temperature on the mole fraction of alcohol according to eq. (9) using  $\Delta H_0=24.7$  kJ/mol and  $T_{m,0}=23.6^\circ\text{C}$ . Note that the theoretical melting temperature should be compared to  $T_c$ , due to the way it was defined in section 3.1.

mol% octanol in membrane	$T_o$ [°C]	$T_c$ [°C]
0	23.5	23.7
2	23.0	23.4
5	21.4	22.6
7	21.5	22.7
10	20.6	22.5
15	17.1	20.5

**Table 4.1.2:** Result of DSC scans on solutions of DMPC multilamellar vesicles containing the listed mol-% octanol within the membrane.

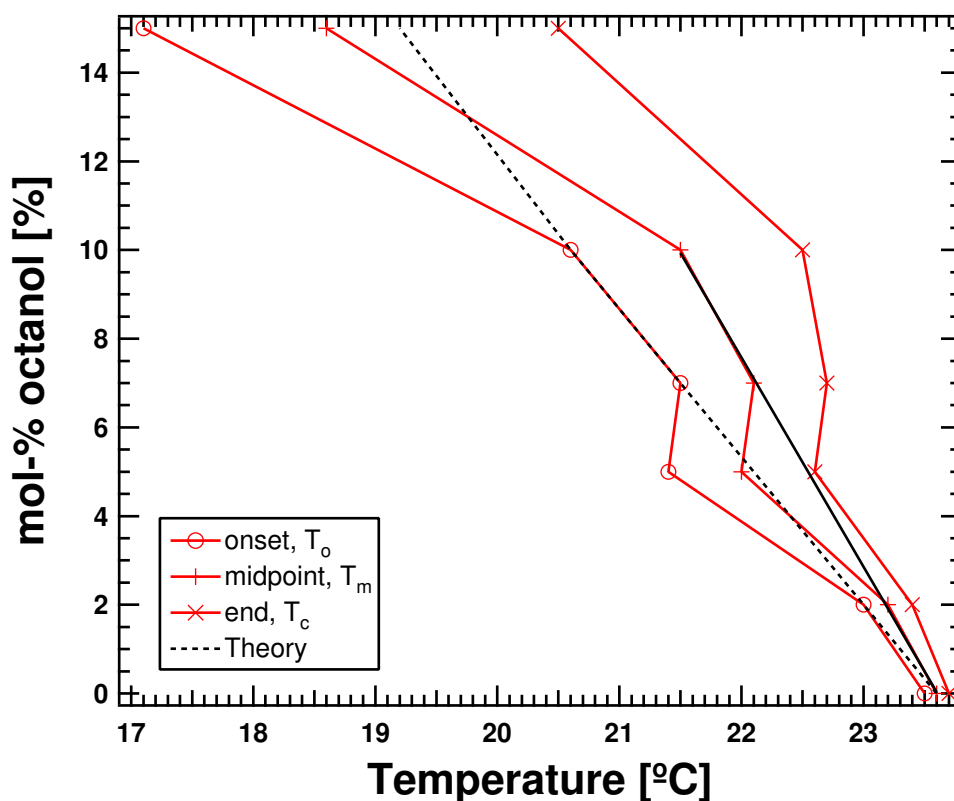


**Figure 4.1.3:** The dependence of the characteristic temperatures of the transition on the amount of octanol in the membrane. Also shown, the transition temperatures predicted by the theoretical calculations. These should be compared to the measured  $T_c$ 's, for reasons given elsewhere.

From Figure 4.1.3 it can be seen that apart from the points for a mol% of 5 and 15, all of the three transition temperatures  $T_o$ ,  $T_m$  and  $T_c$  show a somewhat linear dependence on the mol% of octanol in the membrane as exemplified by the linear fit of  $T_m$  for the values apart from 5 and 15 mol%.

This linear dependence of  $T_c$  on the mole fraction of octanol is in line with the prediction of the simple thermodynamic model presented in the *Theory* section (eq. (9)), since this used the temperature of completion of the fluid phase as the melting temperature. This being said, the theoretically calculated line overestimates the effect of the alcohol, despite the probably too high value of  $\Delta H_0$ .

Whereas the 15 mol% solution arguably is too concentrated to follow this linear dependence, the 5 mol% solution should follow the linear dependence according to the simple model, since both the solution with 7 mol% and 10 mol% seem to fit the linear dependence nicely

Even though the stated mol%'s are uncertain, as described in the section *Estimate of Errors*, they should still be accurate seen in relation to each other, within the error in weighing and pipetting. From Figure 4.1.2 it is clear, that the solutions in general follow the expected behaviour; an increased lowering of the main transition temperature,  $T_m$ , and an increased widening of the transition in general with an increasing amount of octanol. The exception is the graph of the 5 mol% solution which lies on top of the graph of the 7 mol% solution, the two solutions yielding practically the same results for all three of the transition temperatures. Therefore it seems likely, that due to errors in the sample preparation of the 5 mol% solution, this solution is almost identical to the 7 mol% solution. The results from the FTIR spectroscopy presented below support this.

Further it is important to note, that also the determination of the upper and lower transition temperatures,  $T_c$  and  $T_o$ , is uncertain, since there is no precise definition for these, as there is for  $T_m$ . The validity of the estimation method used here is based on its consistency more than a theoretical background.

This being said, the linear dependence observed in Figure 4.1.3 still seems to be significant although only observed over four data points.

## 4.2 FTIR Measurements and Their Correlation With DSC Measurements

FTIR spectroscopy has often been used to monitor lipids going through phase transition by observing the position of the symmetric  $\text{CH}_2$  stretching mode at  $2850\text{ cm}^{-1}$ , due to its sensitivity to the conformation of the hydrocarbon chain [6]. This is illustrated in Figure 4.2.1 where the region of the  $\text{CH}_2$  symmetric stretching mode is shown in a series of spectra of aqueous DMPC solution at various temperatures.

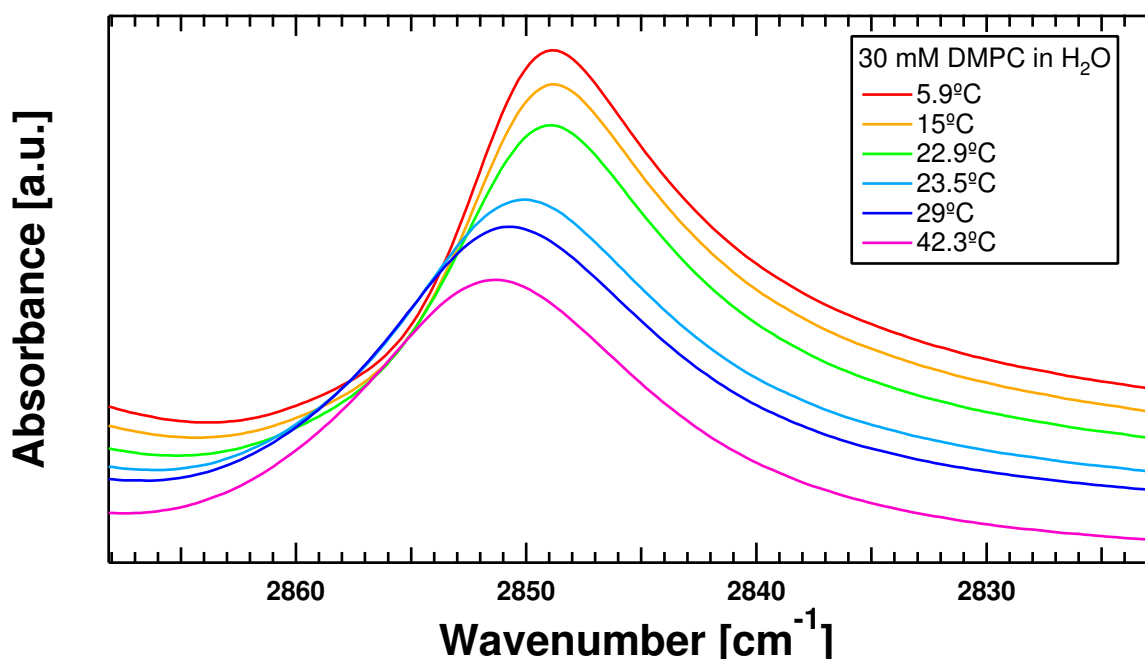


**Figure 4.2.1:** The spectral region of the  $\text{CH}_2$  symmetrical stretching band for a number of temperatures.

The general tendency is clear; the band moves to higher wavenumbers and broadens, with a large part of the overall change taking place within a narrow temperature range.

Figure 4.2.2 shows the temperature dependence of the wavenumber of the 2850  $\text{cm}^{-1}$  stretching peak for DMPC solutions with different amounts of octanol in the membrane as well as pure DMPC. The transition temperature,  $T_m$ , as well as  $T_o$  and  $T_c$ , was determined as described in *Materials and Methods* (Table 4.2.1).

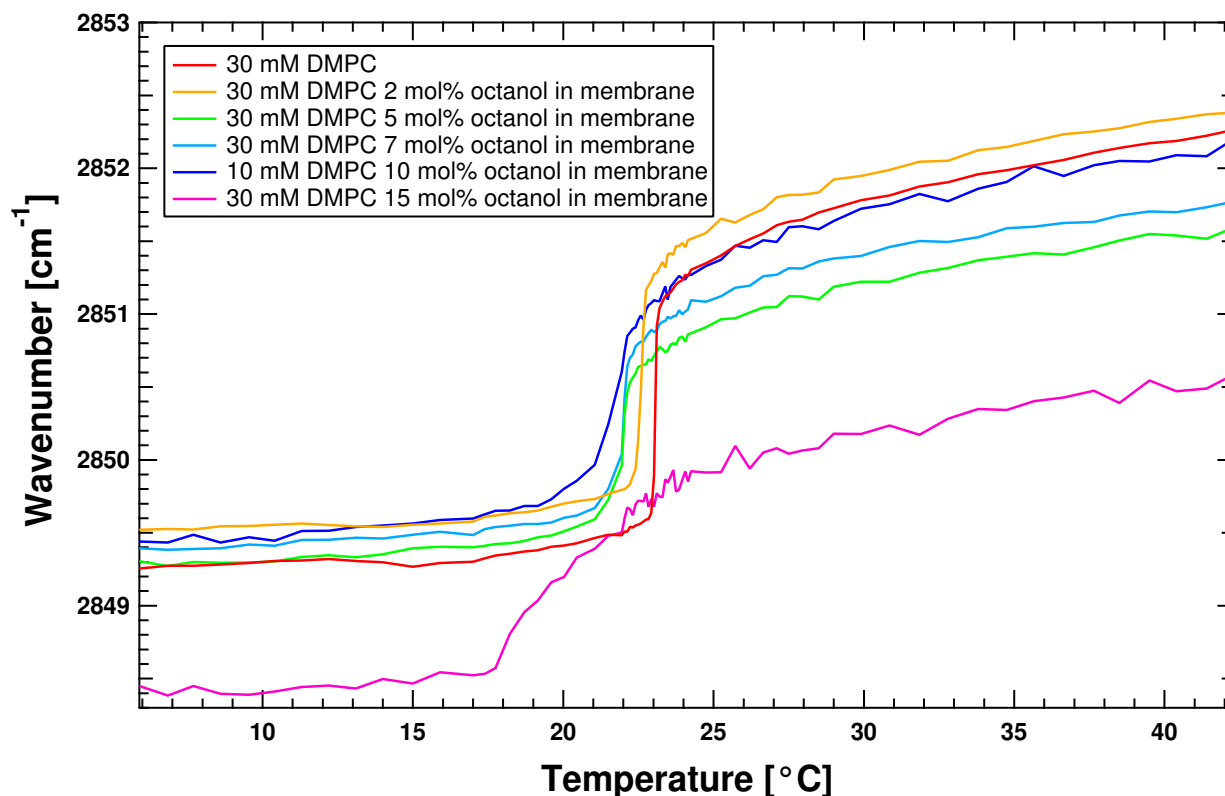


**Figure 4.2.2:** Position of the peak of the  $\text{CH}_2$  symmetric stretching band as a function of temperature for different amounts of octanol in the membrane.

Mol% octanol in membrane	$T_m$ [°C]	$T_o$ [°C]	$T_c$ [°C]
0	23.1	22.9	23.2
2	22.6	22.4	22.8
5	22.0	21.6	22.4
7	22.1	21.7	22.4
10	21.8	20.8	22.8
15	19.5	17.5	21.1

**Table 4.2.1:** Results of FTIR spectroscopy measurements on multilamellar DMPC vesicles containing the listed amount of octanol in the membrane.

As mentioned in *Materials and Methods* the presented curves are peak positions of fits of the measured 2850  $\text{cm}^{-1}$  stretching peaks, since the raw data contained some noise. The noise was probably due to a combination of the limitation on the spectral resolution and inefficient elimination of water vapour from the spectra. The peak positions of the unfitted spectra are shown together with the peak positions of the fitted spectra in Figure A.2 the *Appendix* for each of the solutions in Figure 4.2.2. As can be seen there the curves contain much more noise than can be explained by the

spectral resolution, and large fluctuations in the unfitted peak positions are seen. This means that although the fit is a better estimate of the actual peak position than that obtained from the raw spectrum, the determination of the fitted peak position plots are only certain within  $0.1\text{-}0.2\text{ cm}^{-1}$ . Especially the peak positions at high temperatures are uncertain, and here the uncertainty may be as large as  $0.4\text{ cm}^{-1}$ .

Despite this uncertainty it is clear from Figure 4.2.2, that the peak position shifts about  $2\text{ cm}^{-1}$  for all the solutions, and that the width and temperature of this shift depends on the amount of octanol in the membrane.

Although the effects of octanol on the membrane transition - lowering of the transition temperature,  $T_m$ , and broadening of the transition - qualitatively are the same as assessed by DSC and FTIR spectroscopy, quantitatively they are not. Figure 4.2.3 shows the dependence of the three transition temperatures on the mol% of octanol in the membrane as found by both DSC and FTIR.

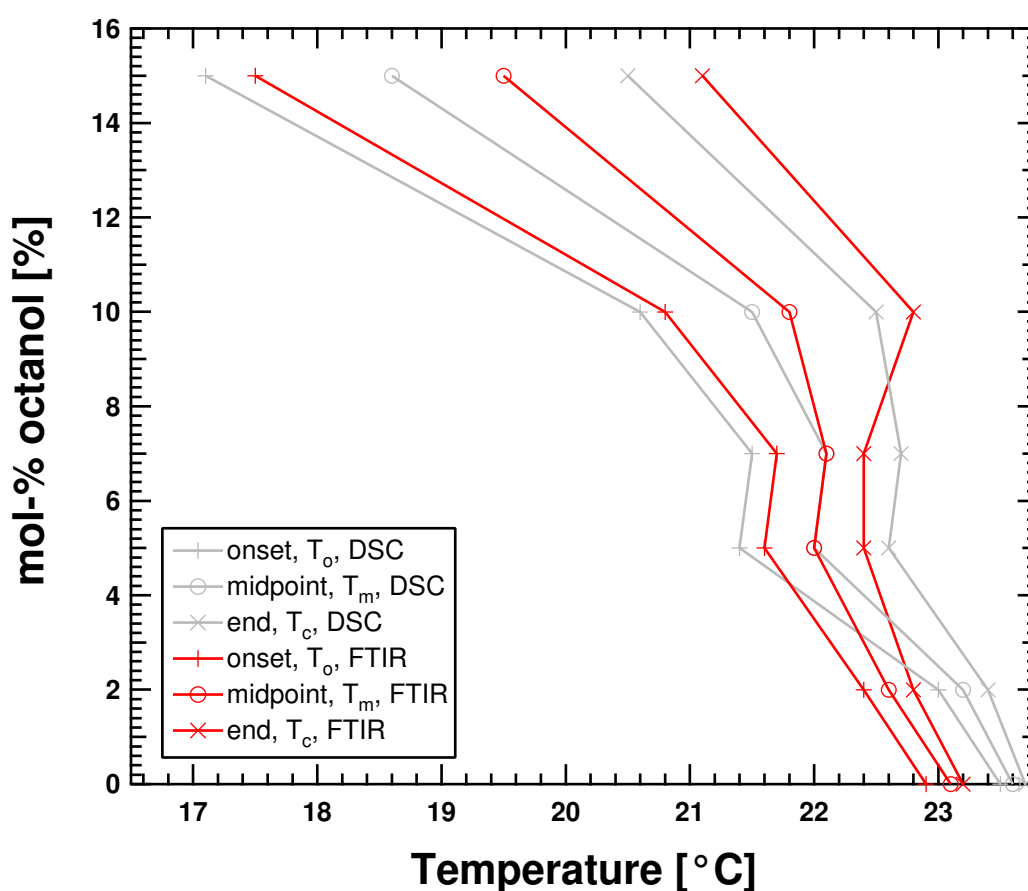


**Figure 4.2.3:** Dependence of the three characteristic temperatures of the transition on the amount of octanol in the membrane. Results from both DSC and FTIR measurements

The different plots do not correspond very well with each other, and it seems like there is a general shift of the temperatures in the FTIR spectroscopy measurements to the lower for low amounts of octanol and to the higher for high amounts of octanol. The melting temperature of the pure lipid, which is known with some certainty to be  $23.6^\circ\text{C}$ , was measured precisely with DSC, while the result was  $23.1^\circ\text{C}$  for the FTIR measurements. Therefore it seems likely that the temperature calibration measurement done on the FTIR experiments as described in *Materials and Methods* has



been inaccurate. This is supported by the fact that the ca. 0.5°C lowering of the  $T_m$  for pure DMPC as measured by FTIR spectroscopy with respect to the DSC measurements, repeats in all of the measured temperatures,  $T_o$ ,  $T_m$  and  $T_c$ , for both the pure DMPC and for the 2 mol% octanol sample. These two samples are the ones where it is relative easy to estimate the temperatures,  $T_o$ ,  $T_m$  and  $T_c$ , from the Figures 4.1.1 and 4.2.2 whereas it for the higher octanol concentration becomes more uncertain. This makes it hard to tell whether the seen discrepancy between the results from DSC and FTIR for higher octanol contents than 2 mol% are due to errors in the temperature calibration measurement or errors in the method for estimating the transition temperatures from the figures.

Both the DSC and the FTIR spectroscopy measurements are said to measure the phase transition of the lipids in the membrane. Therefore it seems likely, that the parameters measured in the two experiments, heat capacity/enthalpy and wavenumber, respectively, show a correlation.

The possible correlation has been tested for the sample of pure DMPC by plotting wavenumber as a function of enthalpy for like temperatures (Figure 4.2.4). In this plot the wavenumbers have been shifted 0.55°C up in temperature due to the observations mentioned above.

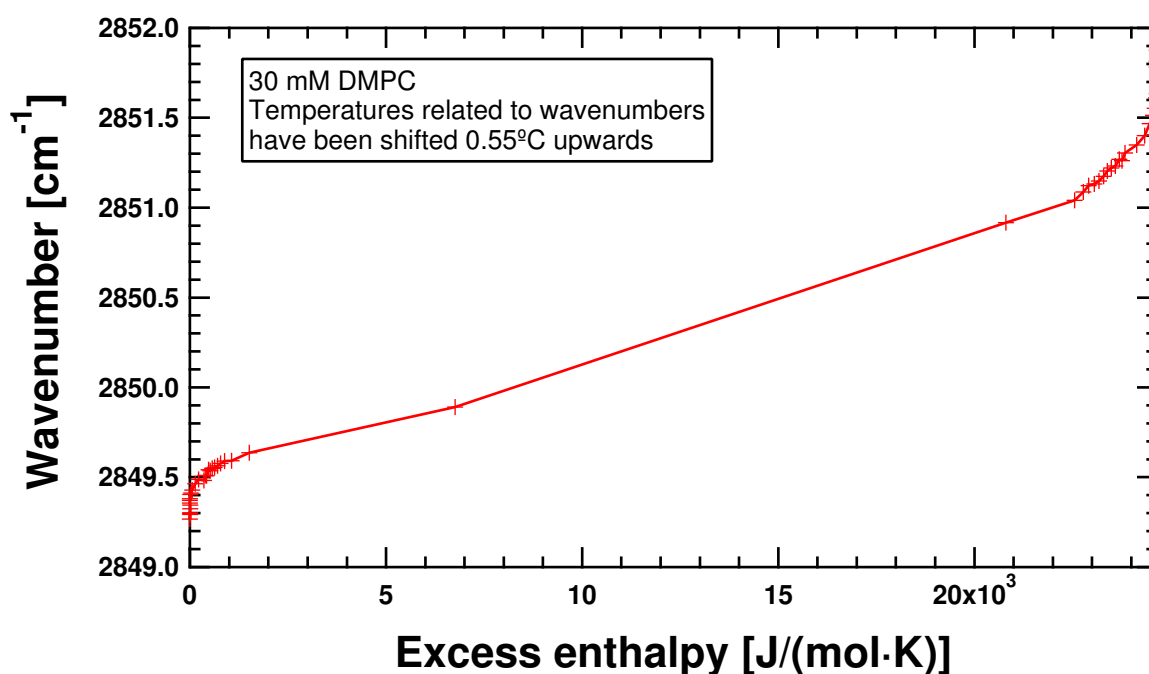


**Figure 4.2.4:** Relationship between the wavenumber of the 2850  $\text{cm}^{-1}$  band and the enthalpy over the temperature range of measurements.

As seen in Figure 4.2.4 there are segments of linear relationship, but not a directly linear relationship between enthalpy and wavenumber over the whole range. The deviation from the linear tendency is strongest for low and in particular high temperatures, where the wavenumber rises while the enthalpy is more or less constant.

### 4.3 Behaviour of Octanol in the Membrane

To monitor the behaviour of octanol in the membrane, dDSPC was mixed with a given amount of octanol. A  $\text{CH}_2$  symmetric stretching band for octanol should now be visible at about 2850  $\text{cm}^{-1}$ , since the same peak in the dDSPC should be located at approx. 2090  $\text{cm}^{-1}$ . Figure 4.3.1 shows that the stretching peaks for the pure deuterated lipid are moved as expected. Figure 4.3.1 also shows the spectrum for the dDSPC containing approx. 7 mol% octanol compared to the spectrum of the pure

deuterated lipid. As can be seen there are only peaks from residual  $\text{CH}_2$  groups in dDSPC at  $2850\text{ cm}^{-1}$  and in general the two spectra seem almost identical.

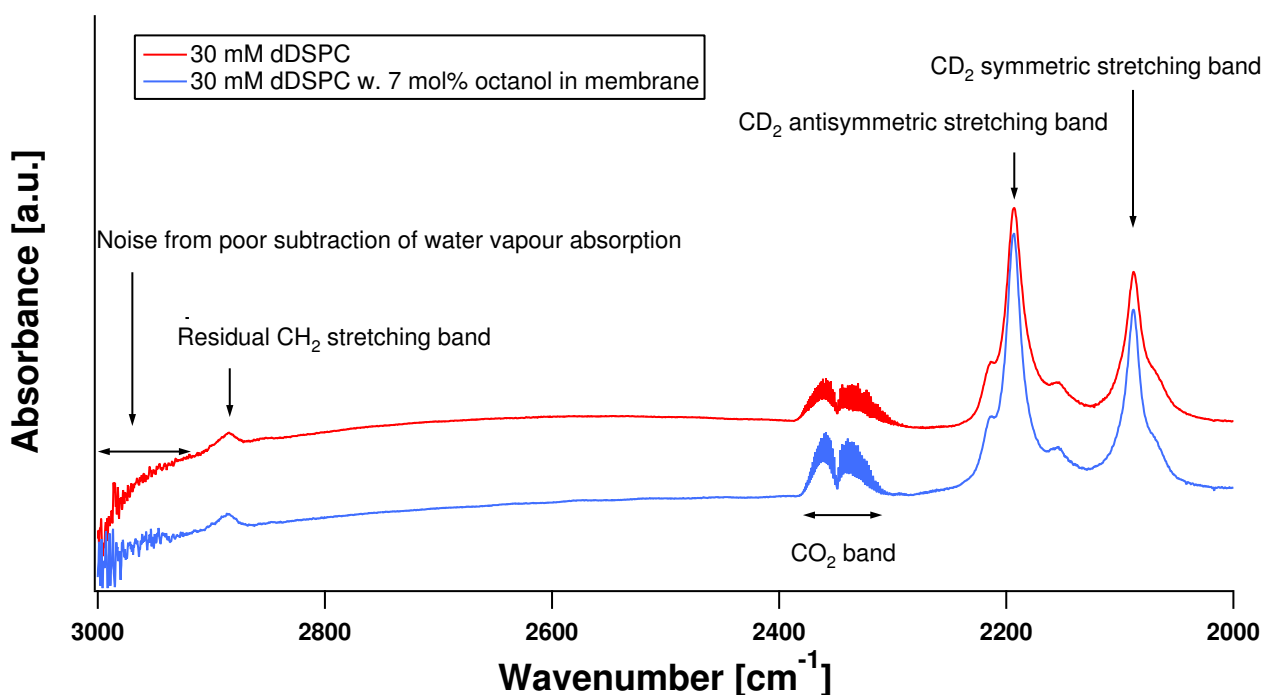


**Figure 4.3.1:** Spectra of pure dDSPC and dDSPC with 7 mol% octanol in the membrane. Shown is the region of the  $\text{CH}_2$  and  $\text{CD}_2$  stretching bands.

That there is octanol present and that it has the expected effect is immediately clear from Figure 4.3.2, where the peak position as a function of temperature is shown for both pure dDSPC and dDSPC containing octanol.

It is clear, that the transition has moved from about  $50^\circ\text{C}$  down to ca.  $48^\circ\text{C}$  in the presence of octanol. The odd behaviour of the peak position in the pure dDSPC in the end of the temperature range was due to evaporation of the solution from the measuring cell, and should therefore be ignored.

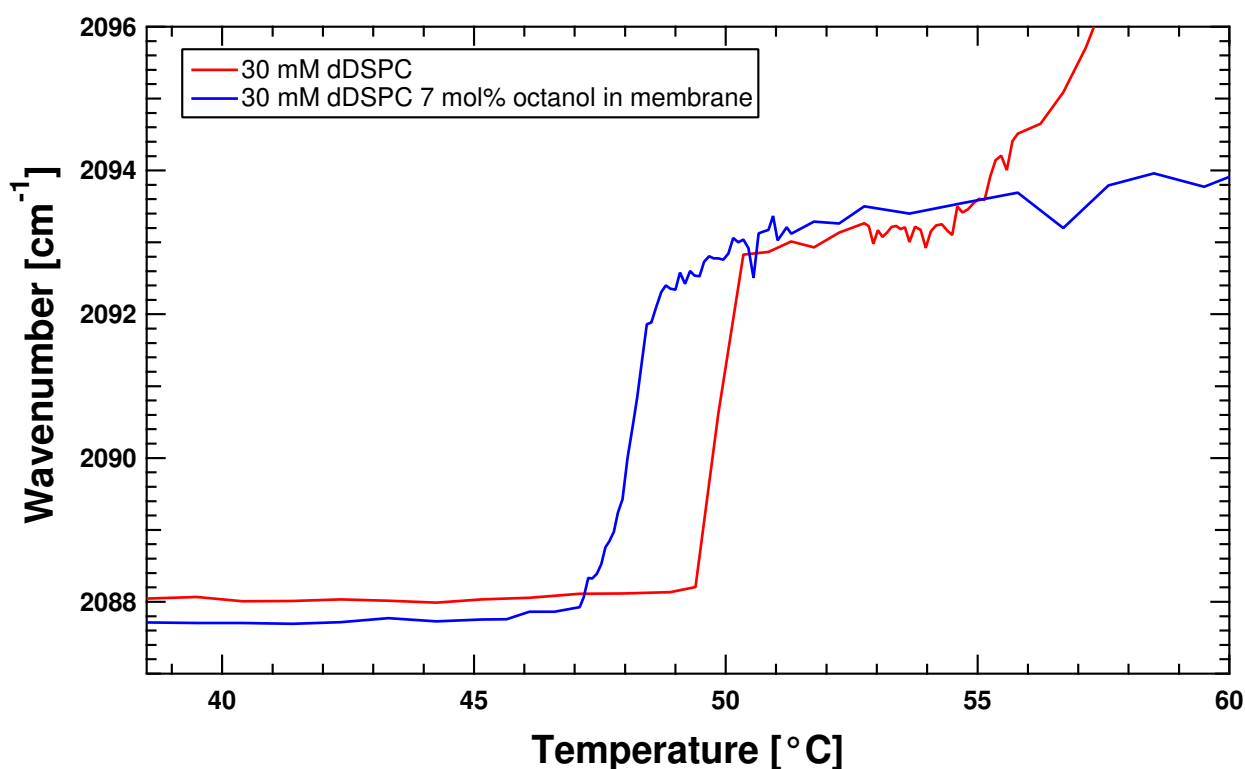


**Figure 4.3.2:** Temperature dependence of the peak position of the CD<sub>2</sub> symmetric stretching peak.

## 5 Discussion

Both the DSC and FTIR spectroscopy measurements showed a widening of the phase transition, which is also seen in the theoretically calculated heat capacity profiles (Figure 4.1.1 and Figure 4.2.3). The reason for this widening is as mentioned a larger effect of the octanol on the onset of the transition than on the end of it as apparent from Figure 4.2.3.

In the simple Hill-model this diminished cooperativity in the transition stems from the fact that a given amount of solute will have a larger diluting effect in a small domain of liquid lipids than in a large domain. Mathematically this is expressed in eq. (9) as a linear dependence of the melting temperature on the mole fraction of anaesthetic in the membrane. According to the model the widening of the transition should be present for all lipids, and thus does not explain the finding that the upper and lower transition temperatures for dipalmitoylphosphatidylcholine (DPPE) upon addition of octanol are affected equally [9].

The measured effect of the octanol on  $T_c$  was smaller than the, from the above mentioned model, calculated effect. In the literature there are examples of measurements reproducing the discrepancy between the measured and the predicted effect of octanol [9], as well as measurements yielding effects in perfect agreement with the theory [8]. The possible tendency of the model to overestimate the freezing-point depressing effect of long chain alcohols has been assigned to a considerable partitioning of long-chain alcohols into the gel-phase lipids [9], [12]. Such a partitioning would diminish the effect of the alcohol in the liquid phase, as can be seen by eq. (7). A measurement of the partition coefficient of octanol between gel-phase DPPC and water found in the literature gave a value of 201 [11], demonstrating that the partitioning into gel-phase lipids might be important in certain systems. In identifying systems in which partitioning into gel-phase lipids might play a role,

it is worth noticing that the difference in partitioning between gel and liquid phases decreases with increasing chain length of alcohol and/or lipid [11].

Another assumption in the simple thermodynamic model is that the solute does not display a melting behaviour of its own. In this study it was attempted to directly monitor the conformational state of the octanol hydrocarbon chain by the use of FTIR spectroscopy. No information regarding the melting behaviour was obtained from these measurements, since there were no CH<sub>2</sub> symmetric stretching bands visible in the recorded spectra. The reason for the missing stretching bands is not clear, and further investigation is needed before any conclusion regarding the possibilities in this approach is drawn. Firstly, the recorded spectra need to have a much better background subtraction, to eliminate the noise seen in the spectra in Figure 4.3.1, since the expected bands would be very small due to the low concentrations of octanol.

Secondly it is possible, that the concentration of octanol needs to be a lot larger than what it was here in order to be able to see the peaks clearly.

Therefore new spectra should be recorded of aqueous solutions of octanol in different concentrations, to see whether the wanted peaks are observable and if so at which concentration.

With respect to the melting behaviour of alcohols it is interesting that decanol has been shown to increase the melting temperature of DMPC but lower it for DPPC, whereas dodecanol raises the transition temperature for both DMPC and DPPC but lowers it for DPPE [9]. For the thermodynamic model this would imply greater solute partitioning into the gel-phase than into the liquid. Based on this observation it has been suggested that decanol and dodecanol in the membrane act as lipids with melting temperatures of about 30°C and 55°C, respectively [9]. Assuming a linear dependence of chain length for such an 'in-membrane' melting temperature, octanol would have a melting temperature in the membrane of ca. 5°C. It would require a membrane of lipids with a melting temperature lower than this, e.g. DLPC, to test such a hypothesis. Based on the homology of the suggested system with the above mentioned it does not seem unlikely, that a freezing point elevation would be observed, indicating melting behaviour of octanol itself.

The simple thermodynamic model contains no energetic terms to account for interaction energies between octanol and lipids or lipids and anaesthetic as well as between gel- and liquid-state lipids. This means that the effects of interactions between gel and fluid lipid domains are not accounted for. The assumptions leading to this are ideal mixing and no interfaces between liquid- and gel-domains, respectively. There is some ambiguity in the literature whether or not the assumption of ideal mixing is justified for the longer alcohols [8], [9], but the assumption of no interfaces is only valid for extremely cooperative systems showing macroscopic phase separation [14]. In general, systems showing high cooperativity are systems with large difference in interaction energy between gel-liquid lipid contacts and the mean of the gel-gel and liquid-liquid lipid contacts [2]. Also the system size matters, since there are different growth rates for surface and area.

The measured effects of octanol can also be accounted for by such energetic considerations. As octanol has a chain length of eight it is much shorter than the lipids in the membrane. This leads to high interaction energy between octanol and lipid, because of an inefficient packing of lipids in presence of octanol. But since the melted lipid is shorter than the gel lipid, the interaction energy between lipid and octanol will be smaller for the melted lipid. Thus the equilibrium between gel and fluid lipid at a given temperature will be shifted in advantage of the fluid lipid, and the transition temperature will shift down. Since there is still interaction energy between octanol and fluid lipid the octanol will tend to aggregate, and its effect on lipid melting will therefore be greatest in the beginning of the transition process where the fluid domains are small, and octanol contact with gel-state lipid is more likely.

The FTIR measurements in this report have confirmed that the method is well suited for studying the phase behaviour of membranes. The obtained results are in line with the theory and the analogue

DSC measurements, although differing in exact values. The measurements also underlined the importance of ensuring perfect background subtraction in order to eliminate the seen uncertainty in measured peak positions, as well as the need of a reliable temperature measurement.

The transition profiles with the fitted peak positions in Figure 4.2.2 showed that it is possible to obtain a reliable peak position from measurements containing considerable noise. As illustrated in *Materials and Methods* this is possible by choosing the fitting interval with care. From the fitted it seems that there is a possibility that the measured wavenumber can be used as more than a diagnostic of the lipids physical state, but due to the level of noise any conclusion must await further investigation. From the obtained data, it seems safe to conclude, that a wavenumber of about  $2850\text{ cm}^{-1}$  is characteristic of the gel phase, whereas a wavenumber above  $2851\text{ cm}^{-1}$  seems to be characteristic for the liquid-crystalline phase.

There is one marked deviation from this apparent rule in the measured data; that is for the sample with 15 mol% octanol in the membrane. As seen in Figure. 4.2.2 the peak position changes from about  $2848.5\text{ cm}^{-1}$  in the gel phase to approx.  $2850.5$  in the liquid-crystalline phase. All of the other samples start around  $2849.5\text{ cm}^{-1}$  and end around  $2852\text{ cm}^{-1}$ , and no general shift to lower wavenumbers with increasing amounts of octanol is seen. The measurement would therefore need to be repeated before anything conclusive could be said about the firmness of the result.

For measuring the temperatures of the onset, midway and completion of the membrane transition, DSC is conclusively the best suited of the two techniques, due to the reliable results and ease with which they are obtained even for a newcomer. Add to this that the obtained heat capacity profile contains immense amount of information readily extracted through application of thermodynamics, and it is clear that DSC is a powerful technique.

The FTIR spectrophotometer on the other hand, has the possibility of measuring any number of different parameters as long as there are distinguishable peaks sensitivity to changes in this parameter in the infrared spectrum. As shown here, the use of deuterated lipids can solve problems with overlapping bands, allowing you to observe two lipids in a mixed membrane separately or to monitor the anaesthetic separately as in this case.

In general FTIR spectroscopy is very well suited to measure the structural change in the membrane, not only in the main transition, but also at the sub- and pretransition by focusing on various bands sensitive to different parameters [6]. The possibility of measuring protein interactions and orientation within the membrane is also one of the techniques trademarks [29].

The attempt to correlate the measured wavenumber of the  $2850\text{ cm}^{-1}$  stretching peak with the measured enthalpy at a given temperature yielded no conclusive results.

Even though the position of the position of the  $2850\text{ cm}^{-1}$  stretching band is said to be dependent on the number of *gauche* conformers in the lipid hydrocarbon chains [6], and we in general would expect the enthalpy of the lipid to depend on the number of *gauche* conformers [2], the expected linear dependence was not seen. The fact that the frequency of these vibrations also depends on intermolecular coupling, librotorsional movements and thermal history of the sample could be the reason that the correlation between enthalpy and wavenumber is not strictly linear [6], [30]. A simpler and more testable reason for not seeing the expected correlation is that the heat capacity profile was baseline corrected. Thus only the enthalpy of the main transition is plotted in Figure 4.2.4, whereas all conformational changes in the given temperature regime are affecting the wavenumber in Figure 4.2.4. A plot of the wavenumber as a function of the non-baseline corrected enthalpy should be made to investigate this possibility.

The model DMPC/dDSPC membranes were chosen for their well-defined physical behaviour and the transitions observed in these membranes are different from transitions in biological membranes in terms of cooperativity and domain size [14]. The goal of this study was in light of what just said,

not to solve the mechanism of anaesthetics, but to measure the well known freezing-point depressing effect of anaesthetics on model membranes. Through these measurements and the study of the field of research as a whole an individual view on the mechanism of anaesthetics would hopefully develop.

From the observed melting temperatures for the DMPC multilamellar membrane we know, that the melting is a continuous process taking place over a defined temperature range even without octanol added to the membrane (Figure 4.1.3). This means that there is a region where liquid and gel-state lipids coexist. By adding anaesthetics the temperature range of coexistence was changed, so that at a given temperature the size and number of liquid and gel domains depended on the amount of octanol (Figure 4.1.3) [14].

In biological membranes small domains, or 'rafts' as they are often called in biology, are believed to play a crucial role by affecting protein diffusion, function and interaction [5], [31]. The mechanism of anaesthetics could be to change the composition/stability of these domains by disturbing the thermal balance, and thereby cell processes that require a specific lipid composition [12].

Speaking against such a randomly domain disturbing model is the observation that octanol administered intravenously to animals resulted in anaesthesia, whereas intravenous injection of hexadecanol resulted in a cataleptic state [9]. This suggests that it is not enough for the solute to go into the membrane to cause anaesthesia, but that it also has to increase the amount of fluid-state lipid in the membrane [9]. Also the fact that application of high pressure, which is known to increase melting temperature of membranes [35], can remove the effects of anaesthesia supports the idea that anaesthetics work through a melting point depression [32], [33]. The way in which a melting point depression should induce anaesthesia is not clear. Though, the observations that ATPase is active in a DMPC membrane ( $T_m \sim 24^\circ\text{C}$ ) down to  $24^\circ\text{C}$ , whereas its activity ceases at  $30^\circ\text{C}$  in a DPPC membrane ( $T_m \sim 41^\circ\text{C}$ ) [9], suggests that an effect on proteins in the membrane is a possibility.

I find it unlikely that anaesthetics bind to the protein directly. If this was the case, the Meyer-Overton correlation would imply that many chemically different substances bound a given protein with exactly the same affinity. That a protein should contain that many binding sites each with the same binding affinity for their specific substrate is inconceivable.

## 6 Conclusion

In this thesis it was found that octanol lowers the melting temperature of both dimyristoylphosphatidylcholine (DMPC) and deuterated distearoylphosphatidylcholine (dDSPC) membranes. The lowering in melting temperature is accompanied by a broadening of the temperature range in which the transition takes place. It was found that the magnitude of the lowering in melting temperature in the case of DMPC was a lot smaller than predicted by a freezing-point depression calculation based on colligative thermodynamics. Further, a correlation between the wavenumber of the  $\text{CH}_2$  symmetric stretching peak at  $2850\text{ cm}^{-1}$  and the excess enthalpy of the system was suggested. Though it requires more measurements before anything conclusive regarding possible correlation can be said. Further studies are also needed to reach a conclusion on the possibility to observe the conformational order of octanol and dDSPC separately though Fourier transform infrared spectroscopy.

Weighing all the gathered informations – written as well as experimental – I believe the most likely mechanism of anaesthetic action is one where proteins in the membrane are affected by anaesthetic molecules dissolved in the membrane. Three things make me draw this conclusion - 1: The relation of the potency of anaesthetics to their oil/water partition coefficient [19], [20]. 2: The similar effects of different anaesthetics on the membrane [16], and 3: The believe that proteins are the functional

units of the cell. The idea of direct interactions with proteins seems unrealistic to me, since this would require a large number of binding sites each binding a specific anaesthetic molecule with common binding affinity.

## 7 References

- [1] R. B. Gennis, *Biomembranes. Molecular Structure and Function*, 1<sup>st</sup> ed., Springer, New York, NY, **1989**.
- [2] T. Heimburg, *Biophysics of Membranes – Biophysics II*, Course material hand-out, **2005**.
- [3] M.W. Tate, E.F. Eikenberry, D.C. Turner, E. Shyamsunder, S.M. Gruner, *Nonbilayer Phases of Membrane Lipids*, *Chem Phys Lipids*. **1991**, 57(2-3):147-164.
- [4] S. J. Singer, G. L. Nicolson, *The Fluid Mosaic Model of the Structure of Cell Membranes*, *Science* **1972**, 175: 720-730.
- [5] M. Edidin, *Lipids on the frontier: a century of cell-membrane bilayers*, *Nature Reviews Molecular Cell Biology* **2003**, 4: 414-418.
- [6] T. L. Bihan, M. Pézolet, *Study of the structure and phase behavior of dipalmitoylphosphatidylcholine by infrared spectroscopy: characterization of the pretransition and subtransition*, *Chem Phys Lipids*. **1998**, 94: 13-33.
- [7] R. Medelsohn, G. L. Liang, H. L. Strauss, R. G. Snyder, *IR Spectroscopy Determination of Gel State Miscibility in Long-Chain Phosphatidylcholine Mixtures*, *Biophysical Journal* **1995**, 69: 1987-1988.
- [8] M. W. Hill, *The effect of anaesthetic-like molecules on the phase transition in smectic mesophase of dipalmitoyllecithin I. The normal alcohol up to C=9 and three inhalation anaesthetics*, *Biochim. Biophys. Acta* **1974**, 356: 117-124.
- [9] A. G. Lee, *Interactions between Anesthetics and Lipid Mixtures. Normal Alcohols*, *Biochemistry* **1976**, 15: 2448-2454.
- [10] A. G. Lee, *Analysis of the Defect Structure of Gel-Phase Lipid*, *Biochemistry* **1977**, 16: 835-841.
- [11] M. K. Jain, L. V. Wray, *Partition coefficients of alkanols in lipid bilayer/water*, *Biochem. Pharmacol.* **1978**, 27: 1294-1295
- [12] N. Janes, J. W. Hsu, E. Rubin, T. F. Taraschi, *Nature of Alcohol on Cooperative Membrane Equilibria*, *Biochemistry* **1992**, 31: 9467-9472.
- [13] J. Stümpel, H. Eibl, A. Nicksch, *X-ray analysis and calorimetry of phosphatidylcholine model membranes. The influence of length and position of acyl chains upon structure and phase behaviour*, *Biochim. Biophys Acta* **1983**, 727: 246-254.
- [14] H. M. Seeger, M. Fidorra and T. Heimburg, *Domain Size and Fluctuations at Domain Interfaces in Lipid Mixtures*. *Macromol. Symp.* **2005**, 219: 85-96.



- [15] M. K. Jain, N. Y-M. Wu, L. V. Wray, *Drug-induced phase change in bilayer as possible mode of action of membrane expanding drugs*, Nature **1975**, 255: 494-496.
- [16] P. Seeman, *The Membrane Actions of Anesthetics and Tranquilizers*, Pharmacological Reviews **1972**, 24: 583-655.
- [17] M. K. Jain, D. G. Toussaint, E. H. Cordes, *Kinetics of water penetration into unsonicated liposomes. Effects of n-alkanols and cholesterol*, J. Mem. Biol. **1973**, 14: 1-16.
- [18] P. Seeman, W. O. Kwart, T. Sauks, W. Argent, *Membrane expansion of intact erythrocytes by anesthetics*, Biochim Biophys Acta. **1969**, 183: 490-498.
- [19] H. H. Meyer, *Zur Theorie der Alkoholnarkose*, Arch. Exp. Path. Phar. **1899** 42: 109-118.
- [20] C. E. Overton, *Studies of Narcosis*, Chapman and Hall **1991**, R. Lipnick, Ed. (Translation of original work published in 1901)
- [21] G. Kreienbühl, B. W. Urban, *Anästhesie in Zürich: 100 Jahre Entwicklung 1901-2001*, T. Patch, E. R. Schmid, A. Zollinger, Eds. (Inst. Anästhesiologie, Universitäts-Spital Zürich, Zürich, **2002**), 10-23.
- [22] B. Antkowiak, *How do general Anaesthetics work?* Naturwissenschaften **2001**, 88: 201-213.
- [23] N. P. Franks, W. R. Lieb, *Where do general anaesthetics act?* Nature **1978**, 274: 339-342.
- [24] R. S. Cantor, *Bilayer Partition Coefficients of Alkanols: Predicted Effects of Varying Lipid Composition*, J. Phys. Chem. B **2001**, 105: 7550-7553.
- [25] L. L. Firestone, J. C. Miller, K. W. Miller, *Appendix. Tables of Physical and Pharmacological Properties of Anesthetics*. From: *Molecular and Cellular Mechanisms of Anesthetics*, S. H. Roth, K. W. Miller, Eds. (Plenum Publishing Corporation, **1986**) 455-470
- [26] H. L. Casal, H. H. Mantsch, *Polymorphic Phase Behaviour of Phospholipid Membranes Studied by Infrared Spectroscopy*, Biochim. Biophys. Acta **1984**, 779: 381-401.
- [27] [http://en.wikipedia.org/wiki/Fourier\\_transform\\_spectroscopy](http://en.wikipedia.org/wiki/Fourier_transform_spectroscopy)
- [28] <http://www.lipidat.chemistry.ohio-state.edu/>
- [29] R. Pascual, M. Contreras, A. Fedorov, M. Prieto, and J. Villalaín, *Interaction of a Peptide Derived from the N-Heptad Repeat Region of gp41 Env Ectodomain with Model Membranes. Modulation of Phospholipid Phase Behavior*, Biochemistry **2005**, 44:14275-14288.
- [30] R. V. Kodati, R. El-Jastimi, M. Lafleur, *Contribution of the intermolecular coupling and librotorsional mobility in the methylene stretching modes in the infrared spectra of acyl chains*, J. Phys. Chem. **1994**, 98: 12191-12197.

- [31] M. Edidin, *The state of lipid rafts: from model membranes to cells*, Annu. Rev. Biophys. Biomolec. Struct. **2003**, 32: 257-283.
- [32] F. H. Johnson, E. A. Flagler, *Hydrostatic pressure reversal of narcotics in tadpoles*, Science **1950**, 112: 91-92.
- [33] A. G. MacDonald, *The effects of pressure on the molecular structure and physiological functions of the cell membrane*, Phil. Trans. R. Soc. Lond. **1984**, 304: 47-68.
- [34] J. K. Kauppinen, D. J. Moffatt, H. H. Mantsch, D.G. Cameron, *Fourier Self-Deconvolution: A Method for Resolving Intrinsically Overlapped Bands*, Applied Spectroscopy **1981**, 35: 271-276.
- [35] H. Ebel, P. Grabitz, T. Heimburg, *Enthalpy and Volume Changes in Lipid Membranes. I. The Proportionality of Heat and Volume Changes in the Lipid Melting Transition and Its Implication for the Elastic Constants*, J. Phys. Chem. B **2001**, 105: 7353-7360.
- [36] M. D. Krasowski and N. L. Harrison, *General anaesthetic actions on ligand-gated ion channels*, Cell. Mol. Life Sci. **1999**, 55: 1278-1303.
- [37] M. K. Jain, *Introduction to Biological Membranes*, Wiley **1988**, New York.
- [38] Picture friendly provided by Thomas Heimburg.

## Appendix

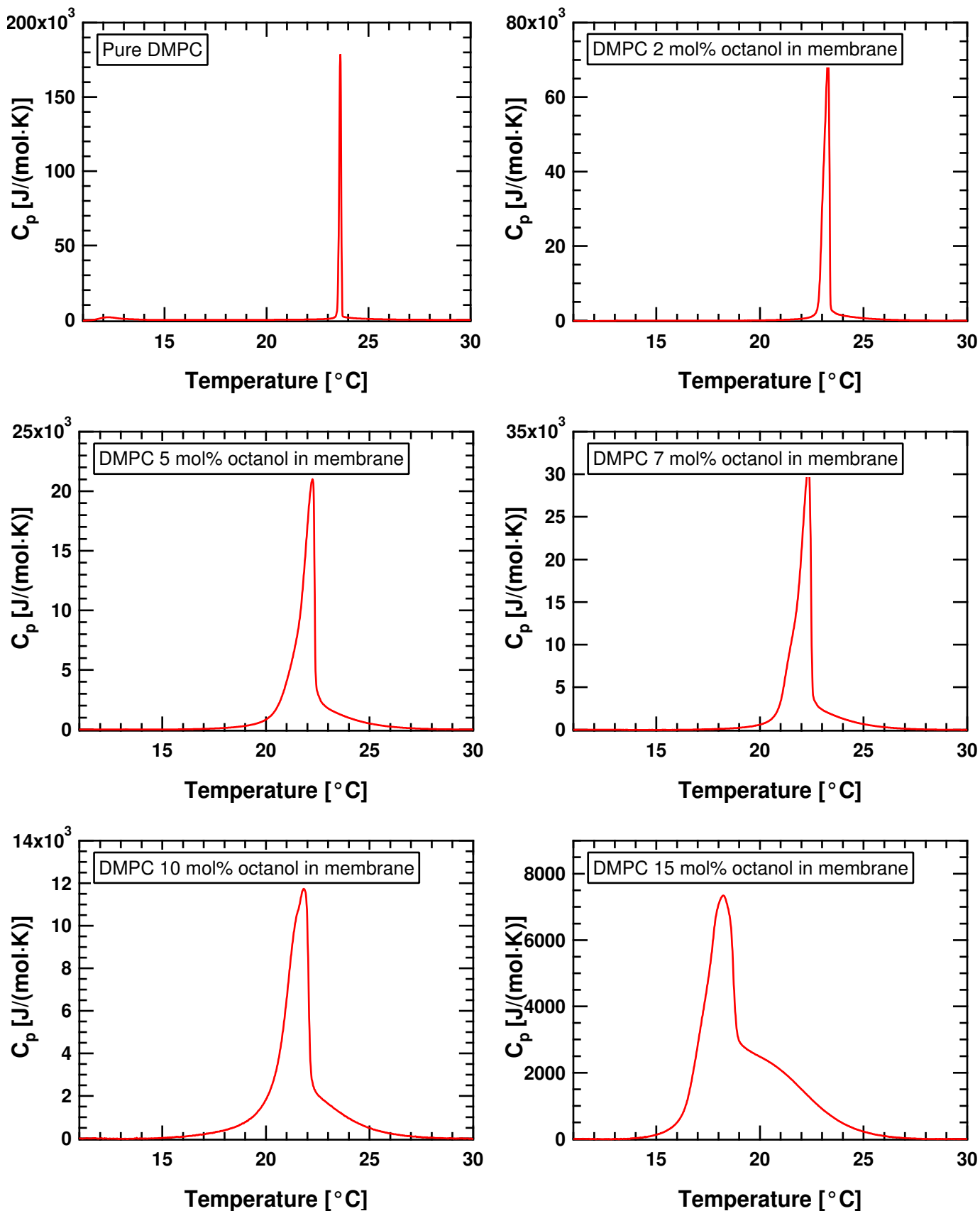
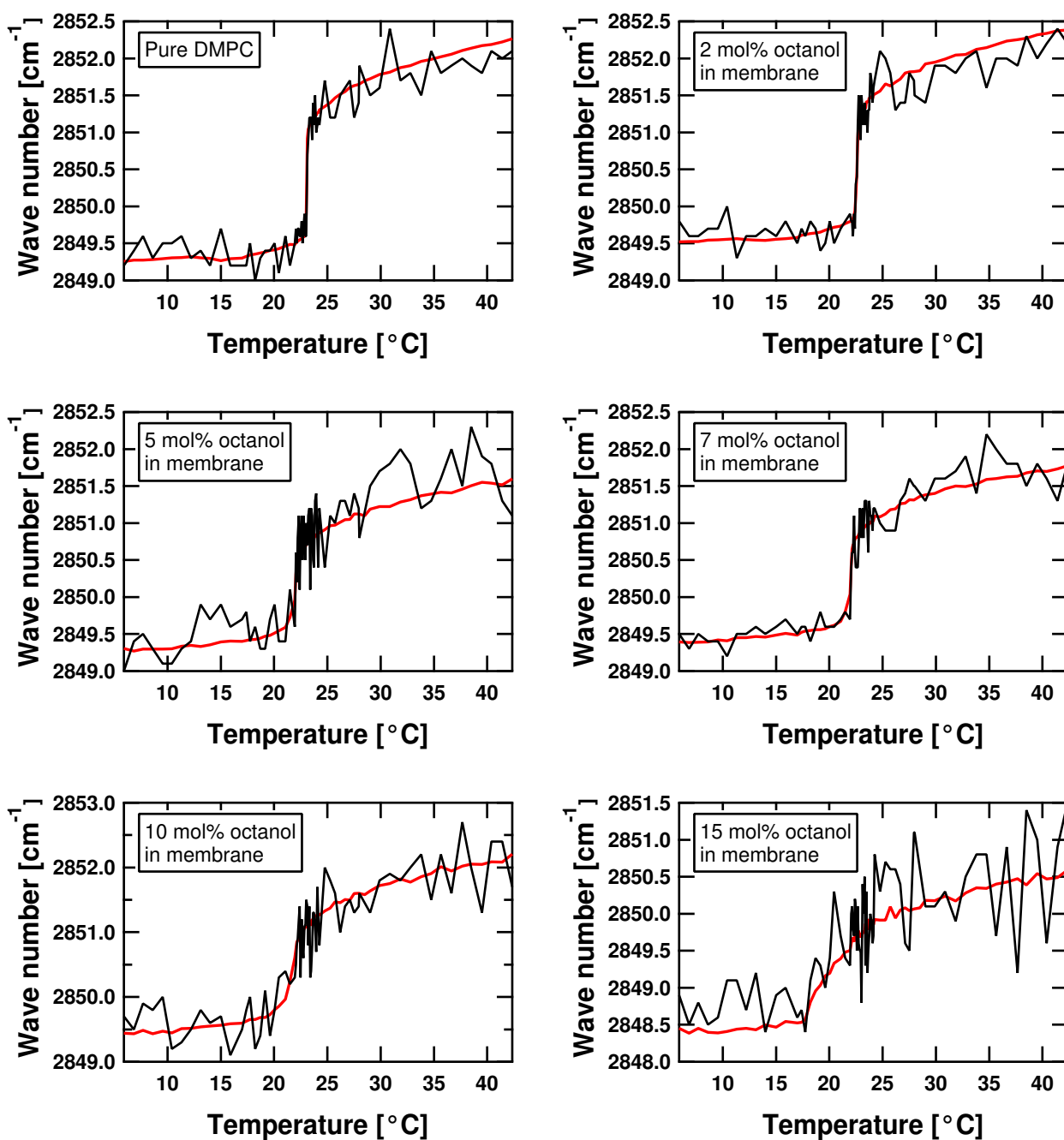


Figure A.1: Excess heat capacity profiles.



**Figure A.2:** Position of the peak of the CH<sub>2</sub> symmetric stretching band as a function of temperature for different amounts of octanol in the membrane. All plots show both the peak positions found from the raw spectral data (black) and the peak positions of the fitted curves (red).